Effects of Charge Motion Control During Cold Start of SI Engines

by

Dongkun Lee

B.S., Mechanical and Aerospace Engineering
Seoul National University, 2003

Submitted to the Department of Mechanical Engineering
in partial fulfillment of the requirements for the degree of

Master of Science in Mechanical Engineering

at the

MASSACHUSETTS INSTITUTE OF TECHNOLOGY

September 2005

Signature redacted

Author .....
Department of Mechanical Engineering
August 19, 2005

Signature redacted

Certified by .....
John B. Heywood
Professor of Mechanical Engineering
Thesis Supervisor

Signature redacted

Accepted by .....
Lallit Anand
Chairman, Department Committee on Graduate Students

To my mother

Effects of Charge Motion Control During Cold Start of SI Engines

by

Dongkun Lee

Submitted to the Department of Mechanical Engineering
on August 19, 2005 in partial fulfillment of the
requirements for the degree of
Master of Science in Mechanical Engineering

Abstract

An experimental study was conducted to investigate the effects of various intake charge motion control approaches on the cold start-up process of a port fuel injected SI engine. Engine experiments were performed to assess the effectiveness of enhanced charge motion on mixture preparation, combustion, and hydrocarbon (HC) emissions. Different charge motions were produced by three different shapes of charge motion control valves (CMCV), which block off 75% of the engine's intake ports.

Cold-fluid steady state experiments were carried out with the CMCV open and closed. Increased charge motion with the CMCV closed was found to shorten the combustion duration, which caused the 50% mass fraction burned to occur up to 5° CA earlier for the same spark timing. By the use of the CMCV, significant improvements in combustion stability (up to 1.5% reduction in COV) and fuel efficiency (up to 8% reduction in ISFC) were achieved with increased levels of spark timing retard due to enhanced air-fuel mixing and relatively faster burning.

Engine start-up experiments were conducted with three different geometric charge motion control valves. The CMCV improved mixture preparation due to increased swirl and tumble intensities, which enhanced fuel distribution and evaporation. Moderate spark retard ($\Delta\theta_{sp}$ = -5°) was found to reduce the engine-out HC emissions during the engine start-up process. Peak engine-out HC emissions with the CMCV closed occurred in the earlier stages of engine start-up process relative to the CMCV open case. Greater fuel vaporization and faster burning rate with the CMCV closed allowed reduced fuel injection and additional spark retard, resulting in significantly reduced HC emissions. The engine-out HC emissions were reduced by 18% during the 0-3 seconds and by 7% during the 3-20 seconds.

Thesis Supervisor: John B. Heywood
Title: Professor of Mechanical Engineering

Acknowledgments

I am ever grateful to God, the Creator and the Guardian, to whom I owe my very existence. He has assured me that He will be with me and pointed out to me that no one has knowledge, power, or importance apart from him.

There have been a number of people without whom this thesis could not have been completed. My deepest gratitude goes out to my supervisor, Professor John Heywood. It has been an honor to be mentored by a leader of such great character, knowledge, and integrity. He has tolerated an incalculable number of questions from me and has weathered that storm beautifully. He has not only taught me about internal combustion engines but also showed me the way of thinking to conduct research.

I would like to thank all of the members of the MIT Engines and Fuels Research Consortium (General Motors, Ford, Daimler Chrysler, Delphi, and Saudi Aramco) for their valuable feedback and support. Special thanks to Dr. Ron Herrin and Dr. Norm Maasshoff of General Motors, who provided the engine, charge motion control devices, and flow testing results. It has been a pleasure working with them, and I hope to continue our working relationship in the future.

The Sloan Automotive Laboratory has been a great place to work, learn, and socialize with fellow students and dedicated MIT employees. Thanks to Michael Gerty and Brian Hallgren for their assistance and companionship for the past two years. It is impossible to name everybody, but I would like to thank those who made my life at the lab interesting and helped me with my research.

I am very fortunate to have wonderful friends with whom I have shared many great times. I would like to extend special thanks to my dream house members (Soon-Jo Chung, Ki Tae Nam, Hyun Jin In, and Jooeun Ahn) for their friendships which have made my life at MIT more enjoyable and truly colorful.

All these years, my family has always been there for me. I would like to express my undying gratitude to my mother, Seok Joong, for her love, prayers, and for providing me a model of how I should live. I also would like to thank my sister, Jin-Ju, for her support and encouragement. Knowing that I have you standing behind me, I will never be afraid to march forward. I love you. Finally, I wish to thank my father, Seung Yeon, who I would give anything to have seen me finish this research project.

Dongkun Lee
August 2005

Contents

List of Figures

List of Tables

Nomenclature

ABDC	after bottom dead center
ATDC	after top dead center
BBDC	before bottom dead center
BDC	bottom dead center
BTDC	before top dead center
CA	crank angle
CMCV	charge motion control valve
COV	coefficient of variation
DAQ	data acquisition
DOHC	dual overhead camshaft
ECM	engine control module
EGR	exhaust gas recirculation
EVC	exhaust valve closing
EVO	exhaust valve opening
FFID	fast flame ionization detector
FID	flame ionization detector
FTP	federal test procedure
HC	hydrocarbon
IAC	idle air control
IMEP	indicated mean effective pressure
IVC	intake valve closing
IVO	intake valve opening
MAP	manifold air pressure
MDS	modular development system
MFB	mass fraction burned
NDIR	non-dispersive infrared
PVC	positive crankcase ventilation
RPM	revolutions per minute
SI	spark ignition
TDC	top dead center
UEGO	universal exhaust gas oxygen

Chapter 1

Introduction

1.1 Background and Motivation

Meeting future, stringent emissions standards will require precise engine control strategies that significantly improve the emissions performance under transient conditions. In particular, greater emphasis is being put upon the cold start-up process where a significant fraction of the total hydrocarbon (HC) emissions can be produced. The use of catalytic converters for aftertreatment is an effective means of reducing tailpipe-out HC emissions from spark ignition (SI) engines. However, the majority of the total HC emissions during the Federal Test Procedure (FTP) are emitted during the first few seconds of engine operation before the catalyst reaches light-off temperature, approximately 250°C. Due to the fact that catalytic converters are essentially ineffective until light-off temperatures are achieved, increased importance is being placed on understanding and improving engine-out HC emissions during the first few seconds of engine operation after cranking.

There are various HC emissions formation mechanisms for SI engines: the filling of crevice volumes with unburned mixture, flame quenching at the combustion chamber walls, oil layer absorption and desorption, incomplete combustion, liquid fuel wetting of in-cylinder surface, deposit absorption and desorption, and air/fuel ratio abnormality [1,2]. During the engine start-up process, these mechanisms play increased roles in determining the engine-out HC emissions. Of particular importance is the influence of the mixture preparation process which can greatly affect these mechanisms. However, it is difficult to achieve appropriate mixture preparation in the cold start-up process due to the unfavorable fuel transportation and evaporation environment such as low port air velocity, initially atmospheric port pressure, and low port and cylinder wall temperatures.

Since only a small portion of injected fuel vaporizes and contributes to the combustible mixture in a cold engine [3,4], the cold start-up process of port fuel injected SI engines generally involves significant over-fueling in the intake manifold. A substantial amount of fuel is injected to overcome unexpected transients as well as poor mixture preparation. This fuel enrichment provides a sufficiently large amount of vaporized fuel so that smooth and robust start-up can be assured. A large portion of this excess fuel, however, does not vaporize and enters the cylinder as liquid [5]. This fuel may be stored in various places in the cylinder (e.g. deposits, oil layers on the cylinder liner, piston top, and cylinder head, or combustion chamber crevices), survive the subsequent combustion process unburned, and come out into the bulk exhaust, where it would significantly contribute to the exhaust HC emissions.

The complex nature of these start-up behaviors requires an improvement in mixture preparation for robust combustion with low HC emissions. The mixture preparation process in contemporary port fuel injected SI engines is significantly affected by intake charge motion, especially during the engine start-up process. It is well known that the in-cylinder charge motion is one of the major factors that controls the air-fuel mixing and combustion process. Since the initial in-cylinder flow pattern is set up by the intake process, enhanced intake charge motion is essential for improving mixture preparation and combustion characteristics, which determine engine-out HC emissions behavior. There are several methods of enhancing charge motion: intake manifold modification, intake valve or cylinder head masking, and charge motion control valves (CMCV). The charge motion control valve is one of the most cost-effective methods for a high level of in-cylinder charge motion.

1.2 Previous Work

Over the past few decades, great efforts have been placed on reducing vehicle emissions. With the development of catalytic converters, the HC emissions in the start-up process of SI engines have become a significant part of the total emissions. A number of studies have been done to investigate the various aspects of the start-up process and reduce the HC emissions with robust combustion. Mixture preparation during the start-up process has been

the focus of previous research. Most of previous studies have concentrated on the effects of fuel metering and liquid fuel behavior on mixture preparation and HC emissions.

In a previous study performed by Henein *et al.* [6], the effect of engine transients on HC emissions was investigated. The initial piston position was found to affect the HC emissions during the cold start-up process. The first cycle fuel metering effect on HC emissions was examined by Castaing *et al.* [7]. The open valve injection was detrimental to the mixture preparation process during the start-up because it caused mixture non-uniformity, directly deposited fuel in the cylinder which increased engine-out HC emissions. There have been some studies investigating the effect of enhanced charge motion on engine performance. In a study conducted by Takahashi *et al.* [8], the use of the CMCV increased the burn rate and combustion stability. More improvement in combustion stability was obtained by optimizing the geometry of the CMCV. Similar research by Nishizawa *et al.* [9] showed that the cold start-up HC emissions were reduced by an electronically actuated CMCV with a high-speed starter and a fast light-off catalyst. Jung *et al.* [10] showed some benefits of the CMCV in the fuel consumption and cam retard at light load conditions. At medium and high load conditions, the CMCV caused an excessive pumping work penalty due to the flow restriction.

1.3 Research Objectives

There has been little study trying to examine the real engine start-up process with the CMCV. Most of the previous experimental studies on enhancing the charge motion for the cold start-up process have been performed under the simulated steady state conditions due to the difficulty of engine control. Therefore, it would be worth to investigate the effects of enhanced charge motion on mixture preparation, combustion characteristics, and HC emissions.

The objective of this research is to quantify the effects of various intake charge motion control approaches on the cold start-up process of a port fuel injected SI engine. Four main tasks were carried out:

- Develop diagnostics to examine the impacts of controlled charge motions on mixture and combustion.
- Identify desirable flow patterns for cold start-up by examining various charge motion control valves.
- Assess the effectiveness of these changes in charge motion on mixture preparation, combustion, and emissions.
- Develop recommendations for improving the charge motion during the engine start-up process.

Chapter 2

Experimental Apparatus and Procedures

2.1 Experimental Setup

2.1.1 Engine and Dynamometer

Experiments were performed on a 2003 model year, 2.2 liter L61 Ecotec (GMX357) engine to investigate the effects of various intake charge motion control approaches on the cold start-up process of a port fuel injected SI engine. The engine was coupled to an eddy current, absorbing only, dynamometer (Froude Consine AE-80). This test setup used the engine starter motor for cranking operation with full control over the engine control modules (ECM). Additional engine specifications are shown in Table 2-1.

Table 2-1 Engine specifications

Ecotec 2.2-liter, 4-cylinder Engine Specifications	
Type	Naturally Aspirated, Line 4
Displacement Volume (cc)	2189
Clearance Volume (cc)	65
Bore (mm)	86
Stroke (mm)	94.6
Connecting Rod (mm)	146.5
Wrist Pin Offset (mm)	0.8
Compression Ratio	10.0:1
Firing Order	1-3-4-2
Valve Configuration	16v DOHC
Valve Timing	IVO: 7° BTDC | IVC: 56° ABDC
	EVO: 49° BBDC | EVC: 19° ATDC
Fuel System	Sequential Fuel Injection

2.1.2 Engine Subsystems and Instrumentation

Air mass flow rate was measured by a thermal mass flow meter (EPI, Series 8000MP). Throttle position control was controlled by a stepper motor (Pacific Scientific SinMax 1.8° motor with 5230 indexer/driver) connected via a cable to the engine throttle body. Incremental movement of the throttle was adjusted by two momentary contact switches with a selectable stepping rate. The positive crankcase ventilation (PCV) system was utilized during the engine operation, but the exhaust gas recirculation (EGR) and secondary air injection system were not used for these experiments.

Fuel was supplied by external fuel pump with an inline filter, accumulator, and pressure regulator. The regulator outlet was connected to the fuel injector rail. A constant fuel rail pressure of 52 psig was maintained for a returnless fuel injection system. Injected fuel mass was calculated from the fuel pulse width duration and pressure differential across the injector.

The coolant temperature was controlled by an external heat exchanger. The engine coolant system was a closed looped system driven by an internal water pump that circulated fluid through the block and cylinder head. The thermostat was removed and the heater core was modified to eliminate the recirculation of coolant within the cylinder head and block. Coolant exited the head and flowed to an external water pump installed in the engine's cooling circuit. The pump outlet was connected to an external heat exchanger and to a coolant reservoir tank before being routed back to the engine. Coolant temperature was varied via a set-point controller that actuated a valve allowing for plant water to flow through an external heat exchanger. The engine oil was not externally cooled and its temperature was measured in the oil pan.

Time-resolved exhaust gas temperatures were obtained from chromel-alumel (type-K) exposed junction thermocouples (0.8-mm bead diameter) with custom radiation shielding. Exhaust air/fuel ratio was measured by a universal exhaust gas oxygen (UEGO) sensor located at the exhaust manifold collector. A Horiba MEXA-700 analyzer interpreted the signal and displayed the air/fuel equivalence ratio.

2.1.3 Engine Control System

The Delco Modular Development System (MDS) [11] was used to control and modify the engine control module (ECM). Specific ECM operations were monitored and recorded by the MDS. This system provided the user control of parameters including the change of calibration data by read only memory (ROM) emulation. A PC was connected to the MDS stack that allowed for internal and external data logging. The stack was composed of several units. The main instrument unit (MIU) was the core of the MDS and contained two embedded processors: the main instrument processor (MIP) and the input output processor (IOP). The computer interface buffer internal logging (CIBIL) provided MDS communication with a computer. The analog conversion module (ACM) contained 8-BNC outputs and 2 instantaneous switches scaled from 0 to 5 volts. A 1MB GMPX Pod was connected to the X-pod that interfaced with the ECM and allowed the ECM's EPROM to be flashed for standalone ECM operation. The shell program allowed the user to have full access to lookup tables and relevant environmental variables. Real-time monitoring and modification of several parameters (RPM, MAP, spark timing, air/fuel ratio, and idle air control (IAC) valve position) was accomplished by using the MDS's external display unit (DU). Full control of the engine was possible using the Delphi Electronics Instrument Tool Suite (ITS) running the Saturn Legacy Software. File handling between the computer and MDS unit was achieved using the ITS software. The program CalTools was used to modify ECM parameters and lookup table variables.

2.1.4 Charge Motion Control Valve

The charge motion control valve (CMCV) device was installed between the intake manifold and intake port. The asymmetrical CMCV (base CMCV) was used for the steady state experiment as shown in Figure 2-1. Three different shapes of charge motion control valves were investigated for the engine start-up experiment in order to better understand the effects of the enhanced charge motion on mixture preparation, combustion, and emissions. All three different CMCVs were made of 1 mm aluminum plate and reduced the port cross sectional area by 75% (i.e. 25% notch area). Since the CMCV device was located upstream of the fuel injector, it did not impede the fuel spray.

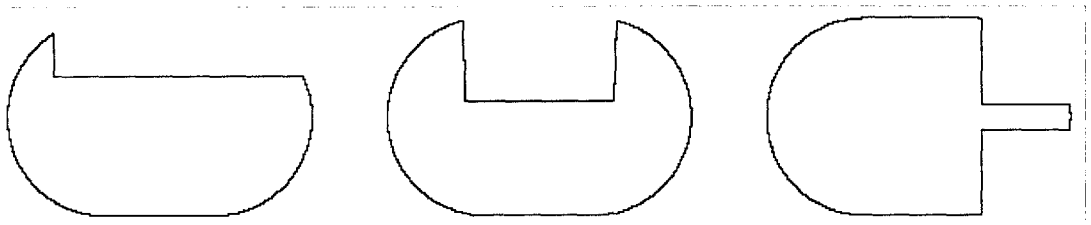

(a) Base CMCV (b) Tumble type CMCV (c) Swirl type CMCV

Figure 2-1 Three different types of charge motion control valves: (a) Base CMCV <CMCV(B)>, (b) Tumble type CMCV <CMCV(T)>, (c) Swirl type CMCV <CMCV(S)>. Flow area was 25% for all three CMCVs.

2.1.5 In-cylinder Pressure measurements

Each cylinder was equipped with a flush-mounted piezoelectric pressure transducer (Kistler 6125A). The cylinder head passage sleeve incorporated an eight-hole flame arrestor to minimize the occurrence of thermal shock. The current signal from the transducer was converted to a voltage signal by a charge amplifier (Kistler 5010B). The transducers were statically calibrated at several pressure points using a dead weight tester. For pressure referencing, an absolute pressure transducer (OMEGA PX-176) was installed in the intake manifold runner that provided better transient response compared to the OEM MAP transducer. In-cylinder pressure was referenced on an individual cycle basis over a 20° CA interval centered around BDC of the intake event, 170° ATDC to 190° ATDC, using the intake manifold runner pressure.

2.1.6 Data Acquisition System

The data acquisition (DAQ) system utilized two DAQ boards from National Instruments installed in a personal computer. The first card (PCI-6071E) acquired 32 differential channels of high-speed signals. The second card (PCI-6024E) was used with a multiplexing chassis (SCXI-1000) and a 32 channel thermocouple module (SCXI-1102) to acquire temperature data from type-K thermocouples. The two boards were operated at different speeds; high-speed data was captured with a frequency of 40000hz (once per 0.025ms), while temperature data was acquired with a frequency of 4000hz (once per 0.25ms). Both

DAQ cards were triggered from signals provided by an incremental encoder (BEI Series H25E) coupled to the engine crankshaft. LabView software was used to create a virtual instrument for data scaling, processing, and logging.

2.1.7 Fast-Response Emissions Analyzers

- Fast-Response HC Analyzer

Time-resolved HC concentrations were measured via a Cambustion HFR400 fast-response flame ionization detector (FID). The FID is the industry standard method of measuring HC concentration. The fast-response FID consists of a main control unit (MCU) and two remote sampling heads. The sample gas is introduced into a hydrogen flame inside the FID. Any hydrocarbons in the sample will produce ions when they are burned. Ions are detected using a metal collector which is biased with a high DC voltage. The current across this collector is thus proportional to the rate of ionization which in turn depends upon the concentration of HC in the sample gas. This fast-response FID has a 10-90% response time of approximately 1 millisecond. A heated transfer sampling line (TSL-H) with a hole diameter of 0.026" was placed at the exhaust port exit, 7 cm from the exhaust valve seats. The fast-response FID was calibrated before and after each experiment using 1500ppmC_3 propane gas (span) and nitrogen gas (zero).

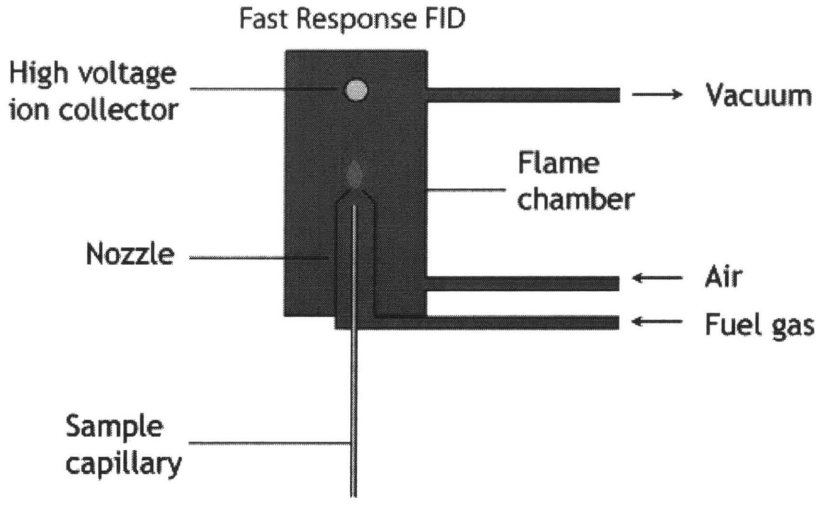

Figure 2-2 Schematic of fast-response FID sampling head from Cambustion [12].

- Fast-Response CO and CO_2 Analyzer

Time-resolved CO and CO_2 concentrations were measured via a Cambustion NDIR500 fast-response non-dispersive infrared (NDIR) detector. The NDIR is the industry standard method of measuring engine exhaust CO and CO_2 emissions. The instrument is a two-channel analyzer with the detectors located in remote sample heads. It measures CO and CO_2 simultaneously from one sample head, providing four streams of data per analyzer. Sample gas from the engine is conveyed through narrow heated capillaries directly into the sample chamber. The optical filters are mounted on a chopping wheel; reference and blank sectors on the chopping wheel correct for minute changes in temperature and IR emitter performance. The instrument gives a T_{10-90} response time of approximately 8 milliseconds. The main control unit is housed in a mobile cabinet with the vacuum pump located in the base. The analyzer is controlled via RS232 or RS485 serial communications from a laptop computer with the installed operating software. The interface provides full control of the instrument including auto-calibration, start-up, self-test, and trouble-shooting and help functions with video assistance. A heated sample probe was located at the exhaust port exit, 7 cm from the exhaust valve seats. Recommended cleaning process was conducted before and after each experiment to remove accumulations from optical windows.

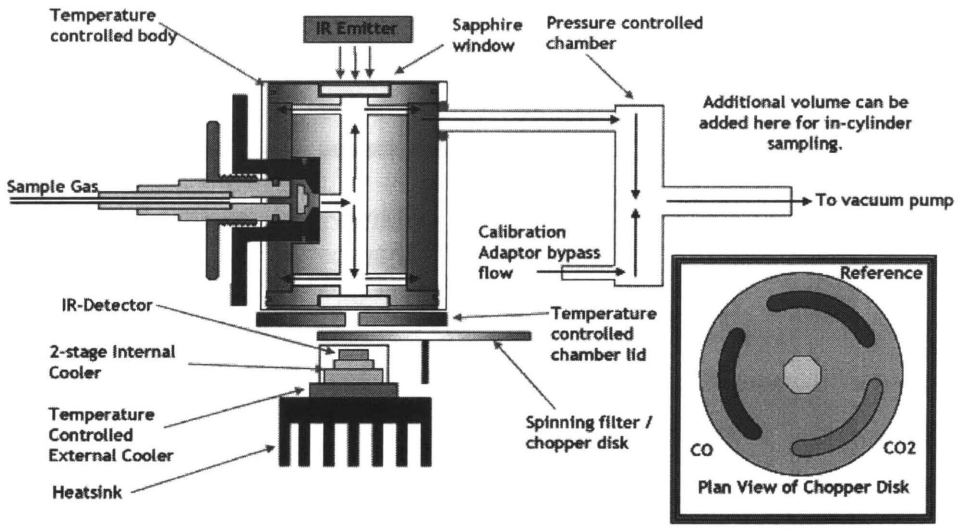

Figure 2-3 Schematic of fast-response NDIR sampling head from Cambustion [13].

2.2 Experimental Conditions and Procedure

2.2.1 Steady State Test Conditions and Procedure

Steady state cold-fluid experiments were performed to understand the basic effects of the CMCV on mixture, combustion, and emissions. In order to simulate the park idle condition, the engine was operated at the condition of 1000 rpm, 2.5 bar Net-IMEP (net indicated mean effective pressure) with the base CMCV open and closed. Spark timing sweeps were conducted with a fixed coolant temperature of 20°C and a stoichiometric air/fuel ratio. The coolant temperature was regulated by an external heat exchanger. The exhaust system, however, was not externally cooled and was allowed to reach a hot stabilized temperature for steady state experiments. A set of 300 cycle data was recorded for each operating condition. All experiments were performed with unleaded test gasoline (UTG), commonly termed "indolene". This is a standardized fuel type typically used for emissions certification and laboratory work. UTG-91 from Chevron Phillips Chemical Company LLC was used for this work to represent the performance of gasoline. The relevant specification of this fuel is in Table 2-2.

Table 2-2 Unleaded test gasoline (Indolene, UTG-91) properties [14].

UTG-91

Property	Typical Value	Specification	Test Method
Specific Gravity at 60/60 °F	0.7350	0.7343 – 0.7440	ASTM D 4052
API Gravity	61.0	Report	ASTM D 1250
Copper Corrosion, 3 h at 50 °C	1	1 max	ASTM D 130
Existent Gum (washed), mg/100 mL	2	5 max	ASTM D 381
Sulfur, ppm	130	1000 max	ASTM D 5453
Reid Vapor Pressure, psia	9.0	8.8 – 9.2	ASTM D 5191
Lead, g/gal	0.0010	0.0050 max	ICP/OES
Phosphorus, g/gal	0.001	0.002 max	ICP/OES
Hydrogen, wt %	13.7	Report	ASTM D 5291
Carbon, wt %	86.3	Report	ASTM D 5291
Carbon Density, g/gal		Report	Calculated
Distillation Range at 760 mmHg, °F			ASTM D 86
Initial Boiling Point	88	75 – 95	
10%	122	120 – 135	
50%	212	200 – 230	
90%	321	300 – 325	
End Point	399	415 max	
Oxidation Stability, min	> 1440	1440 min	ASTM D 525
Heat of Combustion, Net, Btu/lb	18500	Report	ASTM D 240
Composition, vol %			ASTM D 1319
Aromatics	24.0	35.0 max	
Olefins	6.0	10.0 max	
Saturates	70.0	Report	
Research Octane Number	90.8	90.3 – 91.7	ASTM D 2699
Motor Octane Number	82.8	Report	ASTM D 2700
Anti-Knock Index, (R+M)/2	86.8	87.0 max	Calculated
Sensitivity	7.8	7.5 min	Calculated
Oxygenates, vol %		0.0 max	Chromatography
Benzene, vol %		Report	Chromatography

2.2.2 Start-up Test Conditions and Procedure

Engine start-up experiments were conducted with the three different geometric charge motion control valves. Mixture preparation, combustion characteristics, and HC emissions were evaluated with the various fuel injection and spark timing strategies during the first 20 seconds following engine cranking. General Motors provided the target speed-load point during the park idle period of the FTP (0-15 seconds) for this engine. The baseline calibration produced a Gross-IMEP of 3.0 bar and 950 RPM with 0.40 bar MAP and 6°BTDC spark timing. Therefore, the engine was calibrated using the MDS hardware and CalTools software to achieve the target operation condition for the park idle period, 2.5 bar Net-IMEP and 950 RPM. All engine start-up tests were conducted with UTG-91 (Table 2-2) at approximately 20°C environmental conditions. The coolant temperature was initially fixed at 20°C by the external coolant control system.

After each start-up test, the engine was operated and warmed up to a coolant temperature of 70°C to avoid residual fuel build-up in the intake port [15]. After shutdown, the engine was purged by cranking with the injector off for 1 minute. Metal temperatures throughout the engine and exhaust system, then, were force-cooled to ambient temperatures before another experiment was conducted.

Several previous studies showed that the engine start-up behavior is affected by the initial phasing of the piston positions [6,7]. For a 4-cylinder 4-stroke engine, the engine tends to stop with one of the pistons at mid stroke (~90° from the BDC) of compression. Therefore, the piston starting point was fixed at 90°ATDC of the expansion stroke of cylinder #4 to avoid excessive complexity in data analysis.

Engine speed and load were not regulated by the dynamometer controller (Digalog Series 1022A) due to the unstable transient control of the dyno-engine system during start-up RPM flare. The required engine idle load was achieved by utilizing engine accessories with the dynamometer coupled but not absorbing power from the engine. A hydraulic power steering pump and alternator were added to the engine setup to simulate park idle load conditions observed during the first 15 seconds of the FTP. The power steering pump was throttled to 800 psig by the use of a needle valve. The low pressure line was routed through a heat exchanger before returning oil to the reservoir tank. The regulated 14.7 volt output from the alternator was isolated from the 12 volt battery bus by a zener diode and connected to bank of power watt resistors, which had total 0.2 Ohm (three 0.6 Ohm resistors in parallel).

2.3 Analysis Method

2.3.1 Residual Gas Fraction

To calculate in-cylinder air/fuel ratio and engine-out HC mass emissions, it is crucial to be able to estimate the cycle-by-cycle composition of the combustion chamber charge. This charge consists of fresh air, fuel, and residual gas from the previous cycle. The conventional SI combustion process is largely affected by the residual gas fraction. Residual gas in SI engines has a profound effect on emissions, performance, and combustion stability. Residual gas affects the combustion process through its influence on charge mass, dilution, temperature, and flame speed. Residual gas influences combustion mainly by acting as a diluent which decreases the flame speed and temperature of the resulting charge. These effects are especially important for engine idle stability and for HC emissions. Also, interpreting experimental pressure data through chemical energy release and exhaust mass flow analysis requires that the residual gas mass fraction be known. Fox model [16] was used to estimate the residual gas fraction during the engine start-up process since the model is applicable for low to medium engine speeds such that the cylinder pressure does not substantially differ from the exhaust port pressure at IVO. In the model, the contribution of the back flow from the exhaust port to the cylinder during the valve overlap period is accounted for explicitly in terms of a valve overlap factor. For more detailed information regarding the residual gas fraction refer to the Section A.2 in the Appendix.

$$x_r = 1.266 \cdot \frac{OF}{N} \cdot \left(\frac{P_i}{P_e}\right)^{-0.87} \cdot \sqrt{|P_e - P_i|} + 0.632 \cdot \phi \cdot \frac{(P_i / P_e)^{-0.74}}{r_c}$$

2.3.2 Air/Fuel Ratio Determination

Exhaust gas composition depends on the relative proportions of fuel and air fed to the engine, fuel composition, and completeness of combustion. These relationships can be used to determine the operating air/fuel equivalence ratio of an engine from a knowledge of its exhaust gas composition. A general formula for the composition of fuel can be represented as $C_nH_mO_r$. For conventional petroleum-based fuels, oxygen will be absent. Since Indolene

(UTG-91) also has no oxygen in its composition, CH_y (c.f. y = m/n) was used for the following combustion reactions. The overall combustion reaction can be written explicitly as:

$$CH_y + n_{O_2} \cdot (O_2 + 3.773 \cdot N_2)$$
$$+ n_r \cdot \{\tilde{x}'_{CO_2} \cdot CO_2 + \tilde{x}'_{CO} \cdot CO + \tilde{x}'_{CH_y} \cdot CH_y + \tilde{x}'_{H_2O} \cdot H_2O + \tilde{x}'_{NO} \cdot NO + \tilde{x}'_{H_2} \cdot H_2 + \tilde{x}'_{N_2} \cdot N_2 + \tilde{x}'_{O_2} \cdot O_2\}$$
$$\Rightarrow n_p \cdot \{\tilde{x}_{CO_2} \cdot CO_2 + \tilde{x}_{CO} \cdot CO + \tilde{x}_{CH_y} \cdot CH_y + \tilde{x}_{H_2O} \cdot H_2O + \tilde{x}_{NO} \cdot NO + \tilde{x}_{H_2} \cdot H_2 + \tilde{x}_{N_2} \cdot N_2 + \tilde{x}_{O_2} \cdot O_2\}$$

n_{O_2} : moles of O_2 per mole CH_y

n_r : moles of residual gas per mole CH_y

n_p : moles of exhaust products per mole CH_y

$\tilde{x}'$: mole fraction of residual gas component

$\tilde{x}$: mole fraction of exhaust gas component

From the exhaust concentrations of HC, CO, and CO_2, a carbon balance air/fuel ratio was derived. Fox model was combined with this combustion equation in order to provide the mole fraction of residual gas. Throughout the calculation, it has been assumed that the unburned hydrocarbons have the same H/C ratio as the fuel. Since NO_x concentrations are usually sufficiently low during the cold start-up process, NO and NO_2 were negligible for this air/fuel ratio evaluation.

$$\frac{A}{F} = \frac{M_{air}}{M_{fuel}}\left[\frac{W}{C_t} + \left(\frac{C'_T W - C_T W'}{C_T}\right) \cdot n_r - \frac{y}{2}\right]$$

$$C_T = \tilde{x}_{CO_2} + \tilde{x}_{CO} + \tilde{x}_{CH_y} \qquad C'_T = \tilde{x}'_{CO_2} + \tilde{x}'_{CO} + \tilde{x}'_{CH_y}$$

$$W = 1 - \frac{1}{2}\tilde{x}_{CO} + \frac{1}{2}\tilde{x}_{H_2O} + \left(\frac{y}{2} - \frac{1}{n}\right)\tilde{x}_{CH_y} \qquad W' = 1 - \frac{1}{2}\tilde{x}'_{CO} + \frac{1}{2}\tilde{x}'_{H_2O} + \left(\frac{y}{2} - \frac{1}{n}\right)\tilde{x}'_{CH_y}$$

$$K = \frac{\tilde{x}_{CO}\tilde{x}_{H_2O}}{\tilde{x}_{CO_2}\tilde{x}_{H_2}} = \frac{\tilde{x}'_{CO}\tilde{x}'_{H_2O}}{\tilde{x}'_{CO_2}\tilde{x}'_{H_2}}$$

M_{air}, M_{fuel} : molecular weight

2.3.3 Burn Rate Analysis

The burn rate analysis was performed using the in-cylinder pressure data acquired from cylinder #4. A single-zone thermodynamic model [18] incorporating the effects of residual fraction, heat transfer, and crevices was used for the burn rate analysis in order to quantify combustion characteristics with the CMCV open and closed. Fox model was used for the residual gas fraction in this model, heat transfer was handled by the Woschni correlation, and total crevice volume was estimated to be equal to 2% of the clearance volume.

$$\frac{\partial Q_{CH}}{\partial \theta} = \frac{\gamma - 1}{\gamma} p \frac{\partial V}{\partial \theta} + \frac{1}{\gamma - 1} V \frac{\partial p}{\partial \theta} + \frac{\partial Q_{CR}}{\partial \theta} + \frac{\partial Q_{HT}}{\partial \theta}$$

where:

Q_{CH}	Fuel chemical energy
θ	Crank angle
γ	Ratio of specific heat
p	Cylinder pressure
V	Cylinder volume
Q_{CR}	Energy in crevices
Q_{HT}	Heat transfer

Chapter 3

Steady State

Experimental Results

3.1 Charge Motion Overview

Gas motion into and within the engine cylinder is one of the major factors that controls the air-fuel mixing and combustion process. It also has a significant impact on heat transfer. Since the initial in-cylinder flow pattern is set up by the intake process, the intake charge motion plays a critical role in enhancing both the air-fuel mixing and combustion process. During the engine start-up process, it is difficult to achieve an appropriate in-cylinder mixture for robust combustion due to the unfavorable mixture preparation environment such as cold port wall temperatures, initially atmospheric port pressure, and low air velocity. Inappropriate mixture preparation can also cause a high level of HC emissions and a slow combustion process, which decreases combustion stability. Enhanced in-cylinder charge motion, therefore, is essential for mixture preparation, combustion characteristics, and HC emissions during the cold start-up.

Steady state cold-fluid testing was performed to understand the basic effects of the CMCV on mixture, combustion, and emissions. Various parameters were measured at the condition of 1000 rpm, 2.5 bar Net-IMEP. This speed-load point represents the park idle operating condition for this engine.

An asymmetrical charge motion control valve (CMCV), shown in Figure 3-1, was used to promote more rapid air-fuel mixing and also speed up the combustion process in this steady state experiment. The charge motion control valve was installed between the intake port and the intake manifold. This CMCV was made of 1 mm aluminum plate and reduced the port cross sectional area by 75%.

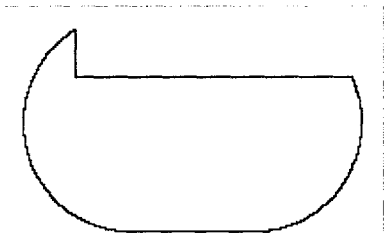

(a) Base CMCV

Figure 3-1 Geometry of charge motion control valve. 25% notch area valve made of 1mm aluminum plate.

3.2 Combustion Characteristics

3.2.1 Combustion Stability

Combustion stability was quantified and investigated in terms of the coefficient of variation (COV) in net indicated mean effective pressure (Net-IMEP). Cycle-by-cycle combustion variations in the combustion process are caused by several factors: variation in gas motion in the cylinder during combustion, variation in the amounts of fuel, air, and residual gas supplied to a given cylinder each cycle, and variation in mixture composition within the cylinder each cycle [1]. Net-IMEP and COV were calculated from in-cylinder pressure data acquired from cylinder #4. A set of 300 cycle data was analyzed for each operating condition. Figure 3-2 shows the COV of the Net-IMEP as a function of spark timing with the CMCV open and closed. With increased spark retardation, combustion stability was found to worsen as combustion occurred in a rapidly expanding cylinder volume. However, significant improvements in combustion stability were achieved with the CMCV closed at late spark timings.

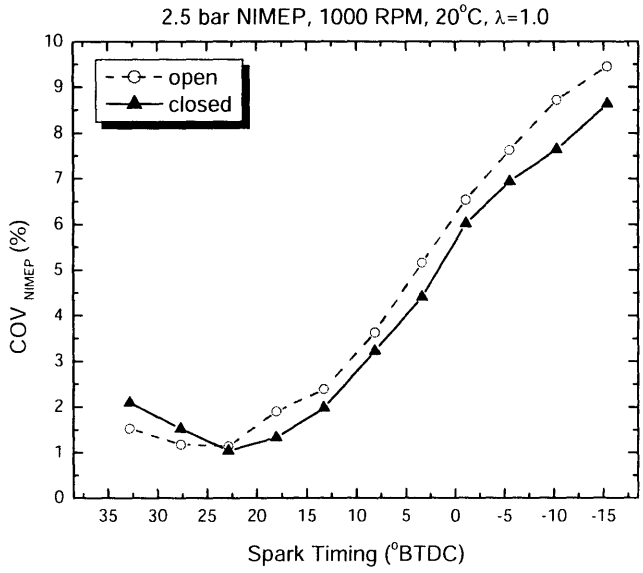

Figure 3-2 COV of the Net-IMEP as a function of spark timing with the CMCV open and closed at 2.5 bar NIMEP, 1000 RPM, and stoichiometric air/fuel ratio with the 20°C coolant.

3.2.2 Burn Rate Analysis

A single-zone thermodynamic burn rate analysis incorporating the effects of heat transfer, residuals, and crevices was used to quantify combustion characteristics with the CMCV open and closed case. Increased charge motion with the CMCV closed was found to shorten the 0-10% and 10-90% combustion duration as shown in Figure 3-3. Figure 3-4 shows that the reduced combustion duration causes 50% mass fraction burned to occur up to 5° CA earlier for the same spark timing.

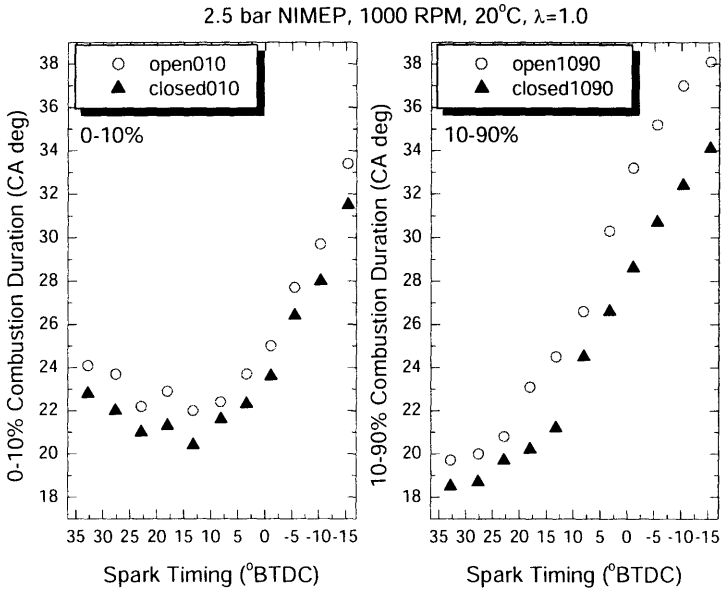

Figure 3-3 0-10% and 10-90% combustion durations as a function of spark timing with the CMCV open and closed at 2.5 bar NIMEP, 1000 RPM, and stoichiometric air/fuel ratio with the 20°C coolant.

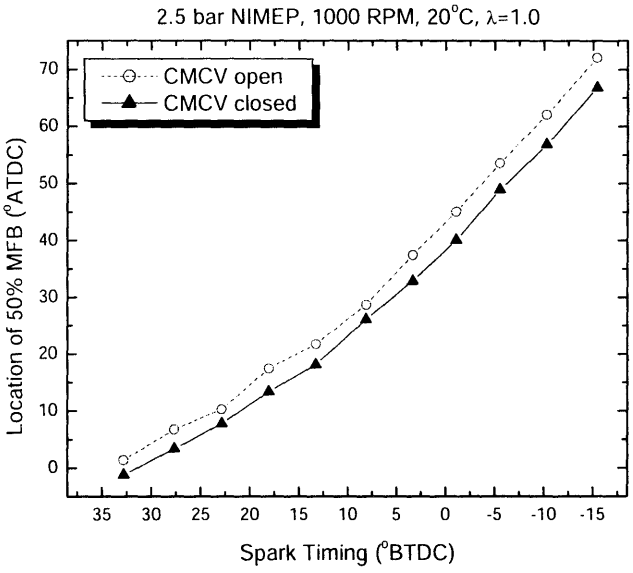

Figure 3-4 Location of 50% MFB as a function of spark timing with the CMCV open and closed at 2.5 bar NIMEP, 1000 RPM, and stoichiometric air/fuel ratio with the 20°C coolant.

3.3 Exhaust Emissions

3.3.1 Exhaust Gas Temperature

The cylinder #4 port exit exhaust gas temperatures were measured with the CMCV open and closed at various spark timings as shown in Figure 3-5. The CMCV decreased the exhaust gas temperature between 5-30°C at a given spark timing, which was attributed to increased in-cylinder heat transfer during combustion. The exhaust gas temperatures were observed to increase with the spark retardation for both the CMCV open and closed case due to the fact that the burned gas is not as fully expanded and does not perform as much work on the piston.

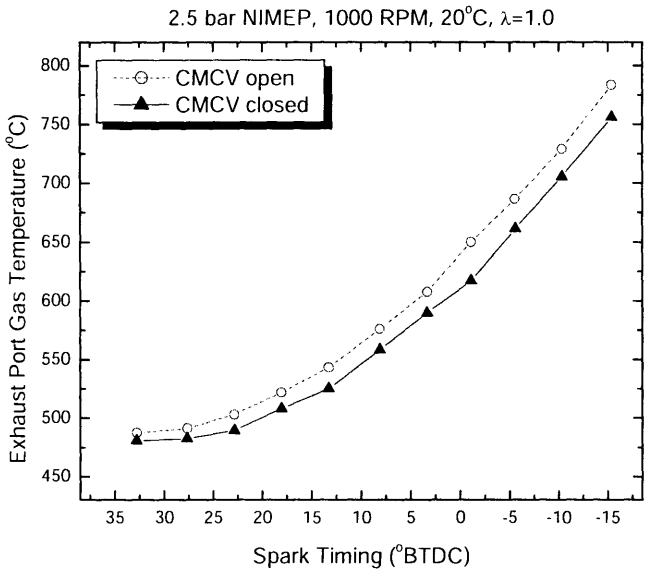

Figure 3-5 Exhaust port gas temperature as a function of spark timing with the CMCV open and closed at 2.5 bar NIMEP, 1000 RPM, and stoichiometric air/fuel ratio with the 20°C coolant.

Since the location of 50% mass fraction burned gives a better indication of when combustion is occurring, it can be used as the indicator of combustion phasing. Figure 3-6 shows that exhaust gas temperatures increased linearly with combustion phasing. At an equivalent phasing, there is a close agreement between the CMCV open and closed exhaust gas temperatures.

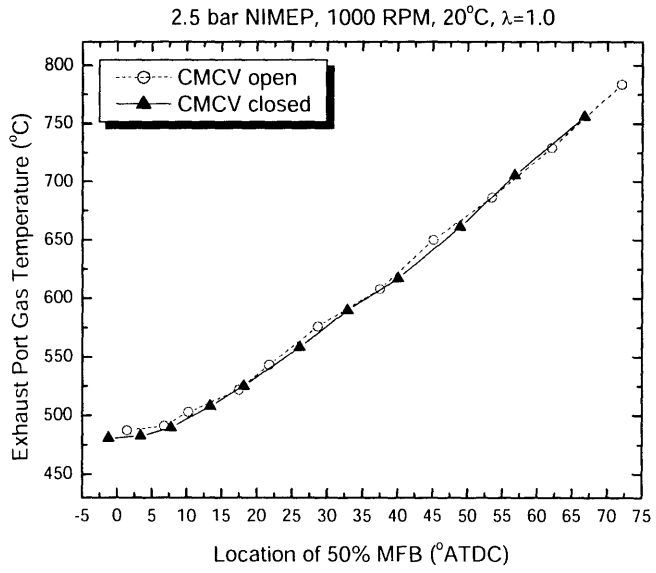

Figure 3-6 Exhaust port gas temperature as a function of 50% MFB location with the CMCV open and closed at 2.5 bar NIMEP, 1000 RPM, and stoichiometric air/fuel ratio with the 20°C coolant.

3.3.2 Exhaust HC Emissions

Figure 3-7 shows the exhaust HC concentrations with the CMCV open and closed for various spark timings. HC concentrations decreased at retarded spark timings mainly due to the reduced crevice volume fraction at peak pressure and increased burned gas temperature at the end of the expansion and during exhaust, which increased oxidation. The exhaust HC concentrations were also investigated as a function of combustion phasing (location of 50% MFB). Figure 3-8 shows that the HC concentrations of the CMCV open and closed cases are almost coincident at a given combustion phasing.

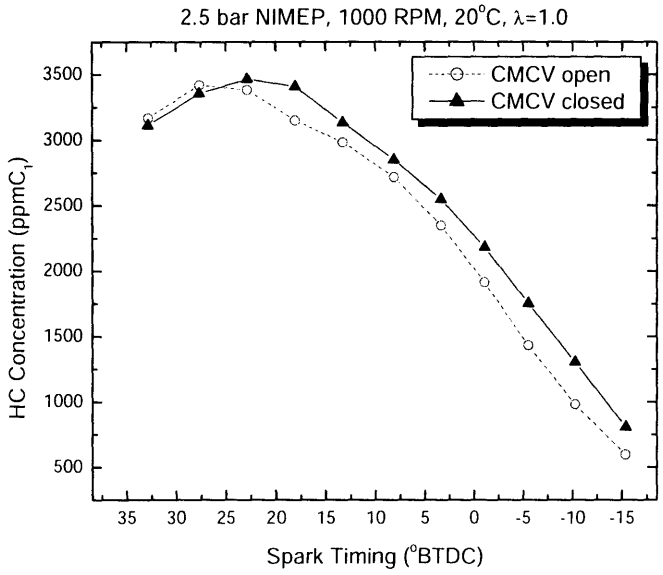

Figure 3-7 Exhaust port HC concentration as a function of spark timing with the CMCV open and closed at 2.5 bar NIMEP, 1000 RPM, and stoichiometric air/fuel ratio with the 20°C coolant.

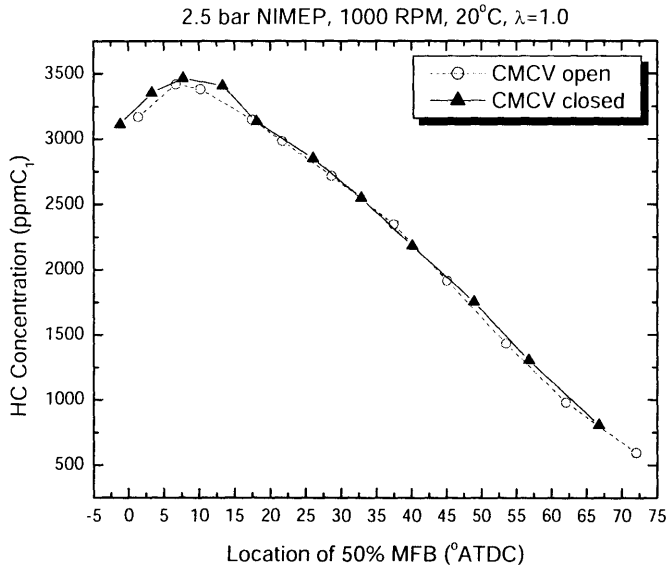

Figure 3-8 Exhaust port HC concentration as a function of 50% MFB location with the CMCV open and closed at 2.5 bar NIMEP, 1000 RPM, and stoichiometric air/fuel ratio with the 20°C coolant.

To achieve the same engine load (Net-IMEP) with late spark timings, the engine's mass flow rate was increased to offset the reduction in work extracted from the burned gas. Therefore, the meaningful representation of the HC emissions is the HC mass flow rate in the steady state. Changes in exhaust mass flow rates were addressed to better interpret the results from the HC concentration data as shown in Figure 3-9.

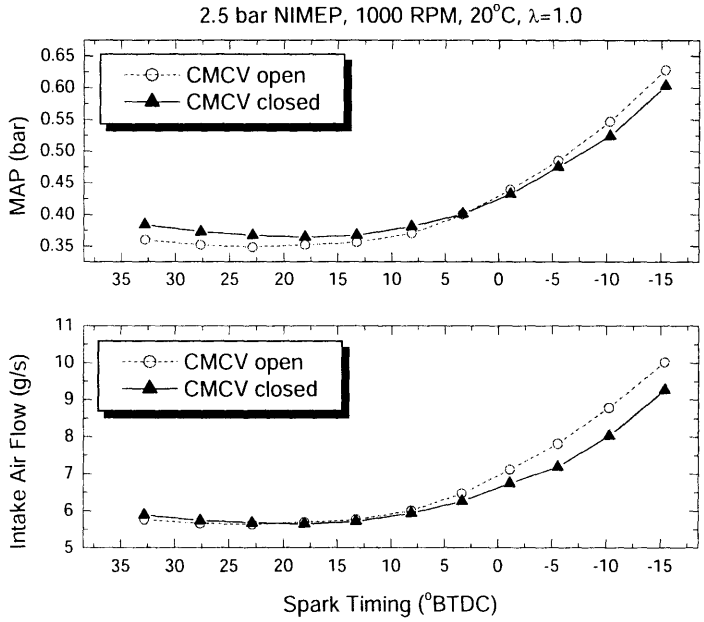

Figure 3-9 MAP and intake air flow as a function of spark timing with the CMCV open and closed at 2.5 bar NIMEP, 1000 RPM, and stoichiometric air/fuel ratio with the 20°C coolant.

Figure 3-10 shows the exhaust HC mass flow rate with the CMCV open and closed for various spark timings. As combustion was phased earlier due to faster burning with the enhanced CMCV generated charge motion at a given spark timing, higher in-cylinder peak combustion pressures occurred, which would increase the mass fraction of the HC trapped in crevice volumes that escaped the oxidation during flame propagation. The important crevice processes occurring during the engine cycle are the following. As the cylinder pressure rises during compression, air-fuel mixture is forced into each crevice region. Since these volumes are thin, they have a large surface/volume ratio; the gas flowing into the crevice cools by heat transfer to close to the wall temperature. During combustion while the pressure continues to rise, air-fuel mixture, depending on engine type, continues to flow into these crevice volumes. After flame arrival at the crevice entrance, burned gases will flow into each crevice until the cylinder pressure starts to decrease. Once the crevice gas pressure is higher than the cylinder pressure, gas flows back from each crevice into the cylinder.

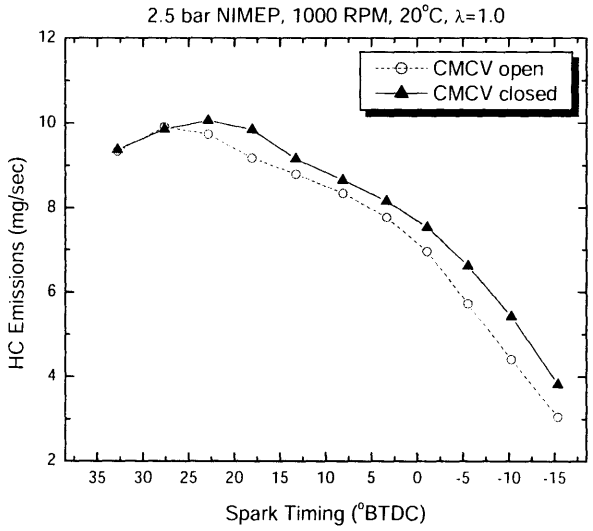

Figure 3-10 Exhaust port HC mass flow rate as a function of spark timing with the CMCV open and closed at 2.5 bar NIMEP, 1000 RPM, and stoichiometric air/fuel ratio with the 20°C coolant.

The exhaust HC mass flow rates were re-plotted in Figure 3-11 at equivalent levels of combustion phasing (location of 50% MFB). The line for the CMCV closed case was almost coincident with the line for the CMCV open case. This indicates that the CMCV gives no noticeable advantage on the exhaust HC emissions at an equivalent combustion phasing in the steady state park idle operation.

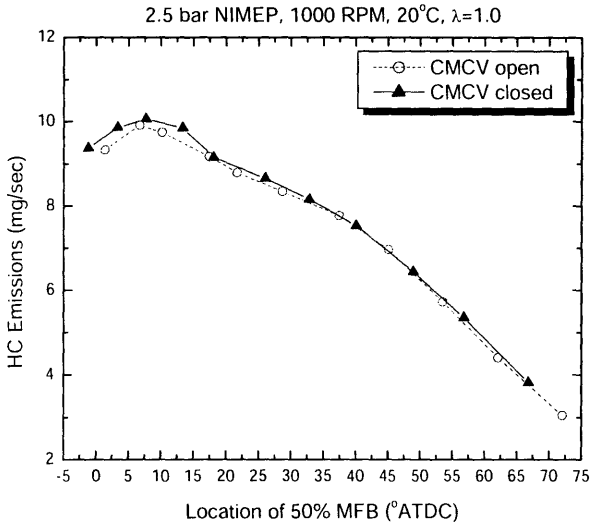

Figure 3-11 Exhaust port HC mass flow rate as a function of 50% MFB location with the CMCV open and closed at 2.5 bar NIMEP, 1000 RPM, and stoichiometric air/fuel ratio with the 20°C coolant.

Chapter 4

Engine Start-up

Experimental Results

4.1 Engine Start-up Overview

Ambient engine start-up is a complicated process that requires delivery of an adequate relative air/fuel ratio around the spark plug gap for a robust combustion event during engine cranking. The engine undergoes severe transients before it reaches the idle speed. Upon the first cylinder firing, the engine accelerates to a speed up to about 1600 RPM, resulting in a rapid decrease in the intake manifold pressure. During the first part of this transient period, spark timing is advanced as engine speed and in-cylinder exhaust gas residuals increase. The engine then decelerates to normal idle speeds during the second part of this transient period; therefore, the intake manifold pressure and spark timing also transition to the idle calibration state. In order to better understand the typical engine start-up behavior, several operating parameters and exhaust emissions were acquired during the first 20 seconds after cranking commenced as shown in Figure 4-1 and Figure 4-2. A substantial amount of fuel was injected into cylinder #4 for the first few cycles to prepare the appropriate in-cylinder mixture for robust combustion. Significantly rich in-cylinder mixture conditions and high transient HC concentrations were also observed during the first few seconds.

The critical processes will be discussed in the following sequence: mixture preparation, combustion, and HC emissions. This is because the intended use of the CMCV is to reduce HC emissions by improving mixture preparation and combustion characteristics. However, the mixture preparation analysis used the engine-out exhaust emissions data as shown in Section 2.3.2.

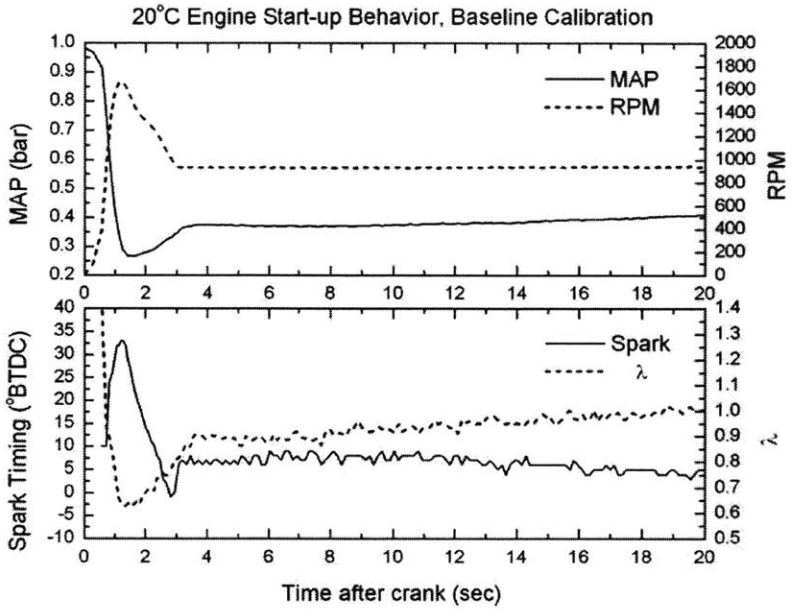

Figure 4-1 **Baseline calibration MAP, RPM, spark timing, and relative air/fuel ratio as a function of time after crank with the CMCV open.**

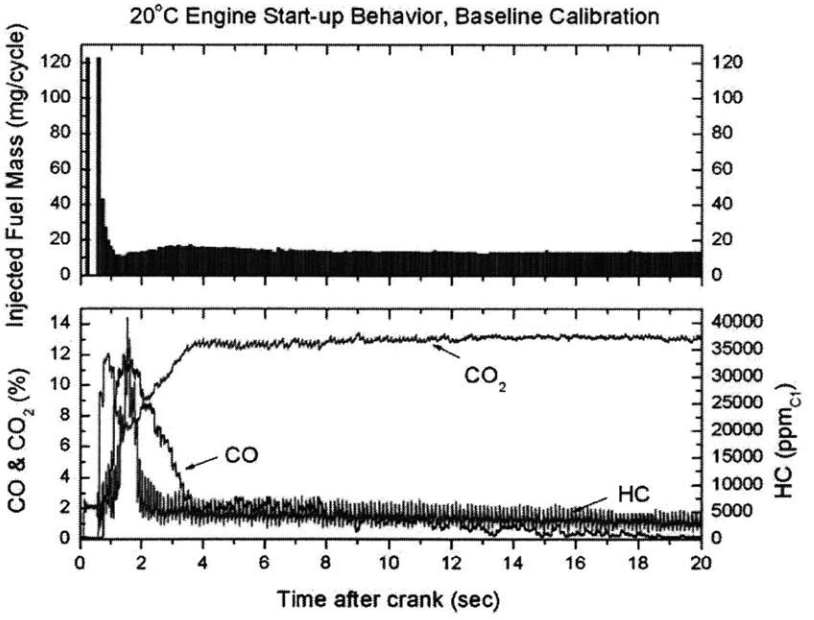

Figure 4-2 **Exhaust gas emissions measured at the exhaust port exit of cylinder #4 as a function of time after crank with the CMCV open.**

During a typical 20°C start-up process, the baseline calibration resulted in an idle speed of 950 RPM and 6° BTDC spark timing at approximately 3 seconds after the onset of engine cranking. The average Net-IMEP of 2.45 bar with 5% COV was obtained during the quasi-steady idle period of 3-20 seconds.

Engine operation in the first 20 seconds showed two clearly distinct periods, which were separated by engine operating conditions around 3 seconds following engine cranking. Thus, in subsequent discussions, the earlier period and the later period are denoted as the transient period and the quasi-steady period, respectively.

4.2 Comparison Results of Various CMCVs

4.2.1 CMCV Overview

In-cylinder charge motion is a transient phenomenon and is developed during the intake process. Gas motion within the cylinder is one of the major factors that controls the air-fuel mixing and combustion process. It is difficult to achieve robust combustion in the start-up process due to the unfavorable mixture preparation environment such as cold port wall temperatures, initially atmospheric port pressure, and low air velocity; each of these conditions is detrimental to fuel vaporization. Therefore, during the start-up process, an increased level of in-cylinder charge motion is helpful for improving fuel vaporization, air-fuel mixing, and tolerance to high levels of residual dilution. Three different shapes of charge motion control valves were investigated to better understand the effects of the enhanced charge motion on mixture preparation, combustion, and emissions. Figure 4-3 shows the three different charge motion control valves named as base CMCV, tumble type CMCV, and swirl type CMCV. All three different CMCVs were made of 1 mm aluminum plate and reduced the port cross sectional area by 75% (i.e. 25% notch area).

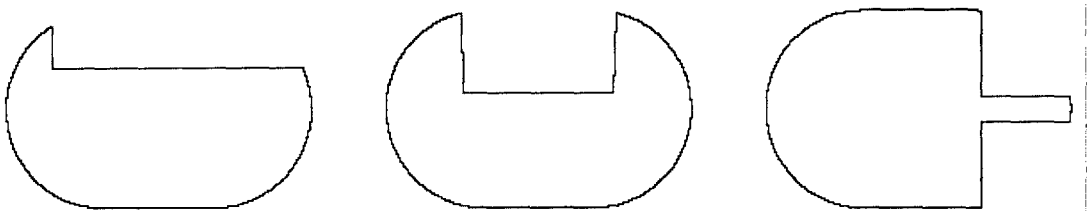

(a) Base CMCV (b) Tumble type CMCV (c) Swirl type CMCV

Figure 4-3 Three different types of charge motion control valves: (a) Base CMCV <CMCV(B)>, (b) Tumble type CMCV <CMCV(T)>, (c) Swirl type CMCV <CMCV(S)>. Flow area was 25% for all three CMCVs.

4.2.2 Mixture Preparation

The task of the engine induction and fuel systems is to prepare an air-fuel mixture that satisfies the requirements of the engine over its operating regime. Mixture preparation is usually discussed in terms of the relative air/fuel ratio. In order to explore this topic here, mixture preparation is defined by the in-cylinder mixture condition just before combustion occurs. The in-cylinder mixture condition just before the start of the combustion was quantified by the calculated in-cylinder relative air/fuel ratio, resulting from fuel vaporization in the port and cylinder produced by the charge motion. In-cylinder relative air/fuel ratio was derived from the carbon based lambda evaluation, which was developed from time-resolved emission measurements, as described in Section 2.3.2.

With the CMCV closed, consistently richer in-cylinder lambda levels were observed from numerous experiments with different amounts of fuel injections. To avoid unnecessarily rich in-cylinder mixture conditions with the CMCV closed, a 4% reduction in fuel injection, compared to the baseline CMCV open calibration, was applied to all the CMCV open and CMCV closed cases for this comparison experiment. The spark timing trajectories, however, remained the same as the baseline CMCV open calibration for all cases. In addition, with the CMCV closed, the idle air control (IAC) stepper positions were varied in order to maintain the same air flow rate as the CMCV open case. Consequently, the same injected fuel and same inlet air mass were delivered to the cylinder, cycle by cycle, for all four different experiments.

In-cylinder relative air/fuel ratio was investigated to evaluate in-cylinder mixture preparation states during the first 20 seconds following engine cranking. In-cylinder lambda was calculated from the exhaust gas concentration data measured at the exhaust port exit of cylinder #4. Figure 4-4 shows noticeable in-cylinder lambda decreases with the CMCV closed. The most significant difference of in-cylinder lambda relative to the CMCV open case was observed with the base CMCV closed.

Figure 4-5 shows the evaporated fuel mass as a function of cycle number during the transient period for various CMCVs. Increased amounts of evaporated fuel mass were observed with the CMCV closed. Figure 4-6 shows the percentage of evaporated fuel to injected fuel during the quasi-steady period. Increased levels of fuel were evaporated with the CMCV closed. The highest fuel evaporation was observed with the base CMCV closed, and approximately 3.5% improvement in amounts of fuel evaporated was achieved with respect to the CMCV open case. The CMCVs were found to improve mixture preparation during the start-up process, and the base CMCV was the most effective from the mixture preparation point of view.

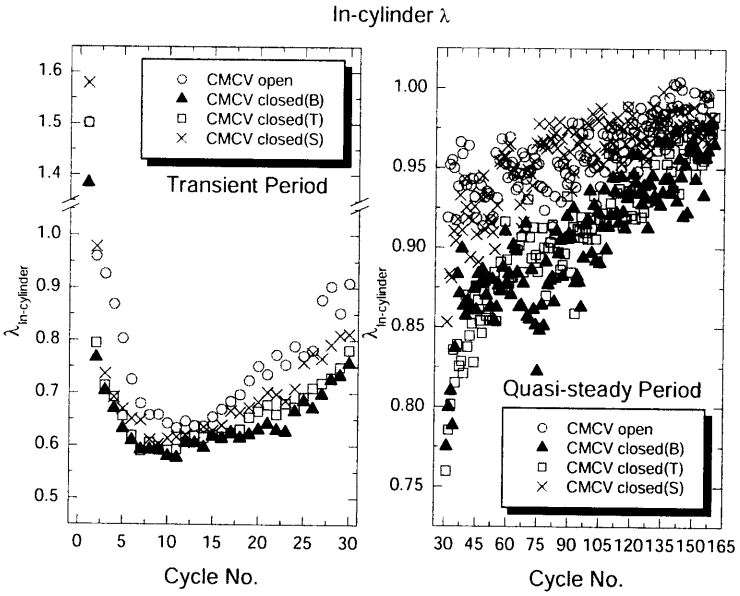

Figure 4-4 **In-cylinder λ as a function of cycle number during the first 20 seconds following engine cranking.**

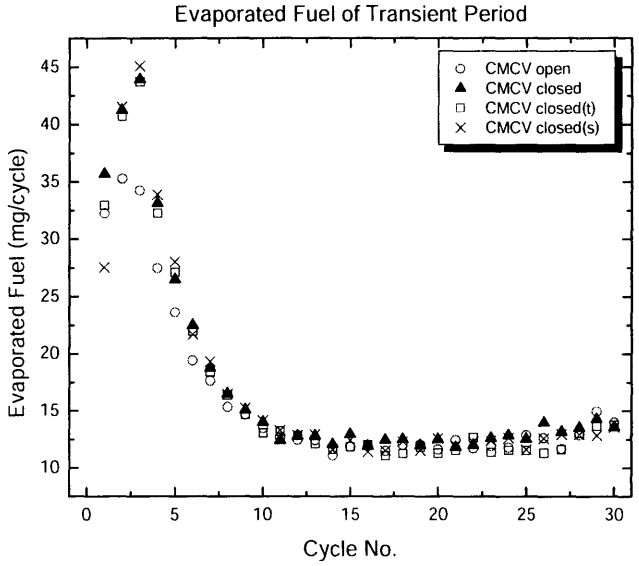

Figure 4-5 Evaporated fuel as a function of cycle number during the transient period for various CMCVs.

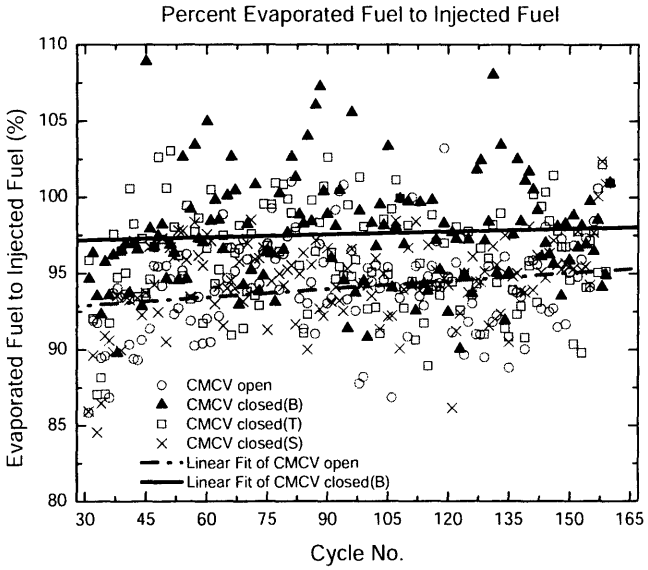

Figure 4-6 Percentage of evaporated fuel to injected fuel as a function of cycle number during the quasi-steady period for various CMCVs.

4.2.3 Combustion Characteristics

Combustion stability was investigated qualitatively during the transient period, and was quantified by the COV of the Net-IMEP during a quasi-steady period. Net-IMEP was calculated from in-cylinder pressure data acquired from cylinder #4. More stable Net-IMEP was observed in all three CMCV closed cases compared with the CMCV open case during the transient period as shown in Figure 4-7. During the quasi-steady period, the COV of Net-IMEP was also decreased with the base CMCV and the swirl type CMCV; a COV of 5.2% and of 5.5% were obtained, respectively, while the CMCV open case yielded a COV of 5.9%. The combustion stability, however, slightly worsened with the tumble type CMCV up to a COV of 6.2%.

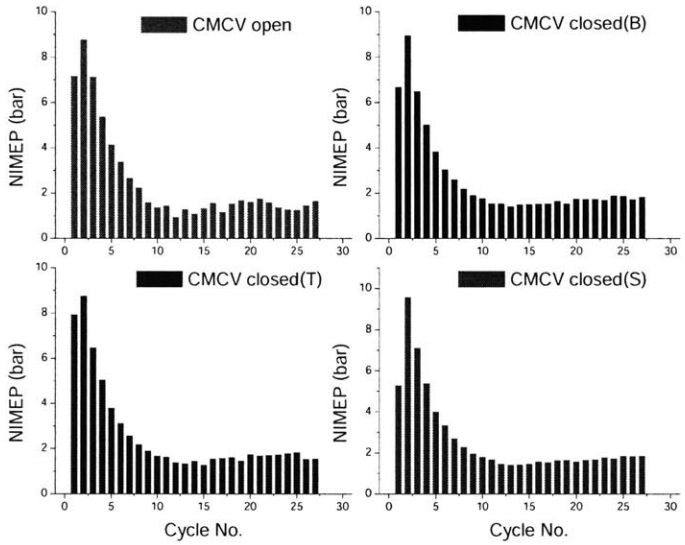

Figure 4-7 Net-IMEP as a function of cycle number during the transient period for various CMCVs.

Burn rate analysis was conducted on the 0 to 20 seconds after cranking. The flame-development angle (0-10% energy-release fraction) and rapid-burning angle (10-90% energy-release fraction) were investigated with the CMCV open and with the various CMCVs closed. It is known that the flame development process is primarily influenced by the mixture state, composition, and motion in the vicinity of the spark plug. The rapid burning stage, during which the major portion of the charge burns as the flame propagates across the chamber, is obviously influenced by conditions throughout the combustion chamber.

The 0-10% and 10-90% combustion durations were shortened with all three different CMCVs as shown in Figure 4-8 and Figure 4-9. In particular, the 0-10% and 10-90% combustion durations were significantly reduced with the CMCV closed during the transient period. There are two plausible mechanisms for these faster burning processes. First, differences in in-cylinder mixture composition, resulting from the enhanced mixture preparation, could affect the combustion duration. On the other hand, differences in gas motion in the vicinity of the spark plug, resulting in differences in motion of the flame kernel during the early stages of development, could also affect the combustion duration.

Least square fit lines for the CMCV open and the base CMCV closed case were added to Figure 4-9 for a more clear illustration. Significant reductions were also achieved with the CMCV closed during the quasi-steady period, due to the combined effect of richer in-cylinder mixture and enhanced gas motion within the cylinder, while the injected fuel mass and spark timing trajectories remained the same for all cases.

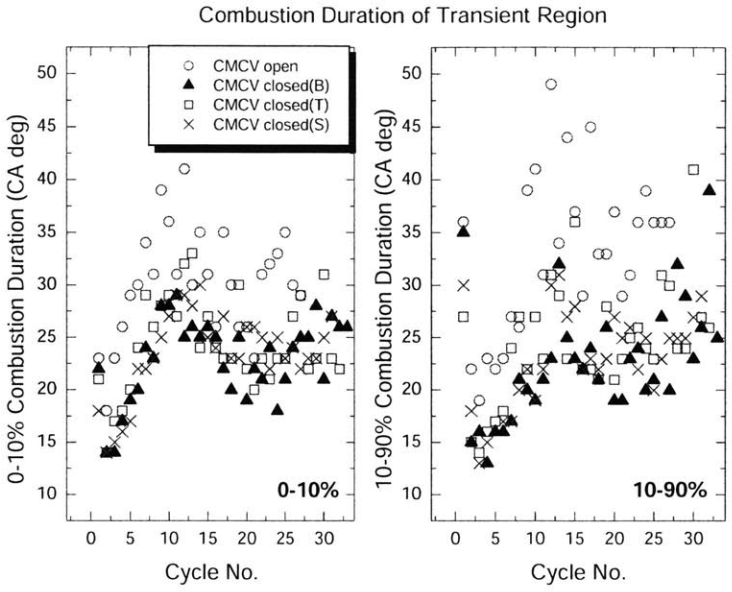

Figure 4-8 0-10% and 10-90% combustion durations as a function of cycle number during the transient period for various CMCVs.

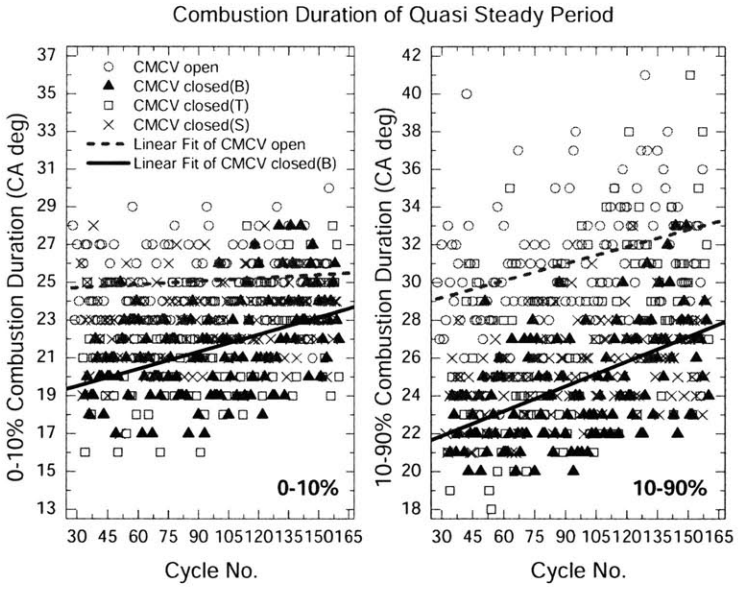

Figure 4-9 0-10% and 10-90% combustion durations as a function of cycle number during the quasi-steady period for various CMCVs.

4.2.4 Exhaust Emissions

Time-resolved cylinder #4 exhaust port exit HC, CO and CO_2 concentration data were taken for the first 20 seconds of engine operation. During the transient period, high HC and CO emissions were observed due to the rich in-cylinder mixture condition and the increased charge dilution. As the engine accelerated, the intake manifold pressure decreased to a low value of about 0.26 bar, which increased the residual gas fraction due to the increased backflow during the valve overlap period. The highest HC mole fraction occurred around cycle #13 where the intake manifold pressure dipped to its minimum value. As the intake manifold pressure started to increase to the idle calibration condition, there was a progressive drop in HC mole fraction.

Using the same fuel injection and spark timing trajectories, higher levels of engine-out HC emissions relative to the CMCV open case were observed with all three different CMCVs. There were several plausible reasons for the trends shown in Figure 4-10 and Figure 4-11. Richer in-cylinder mixture conditions with the CMCV closed cases mainly produced higher engine-out HC emissions. As combustion was phased earlier due to faster burning with the enhanced charge motion, higher in-cylinder peak combustion pressures occurred and also increased the mass fraction of the HC trapped in crevice volumes that escaped the oxidation during flame propagation.

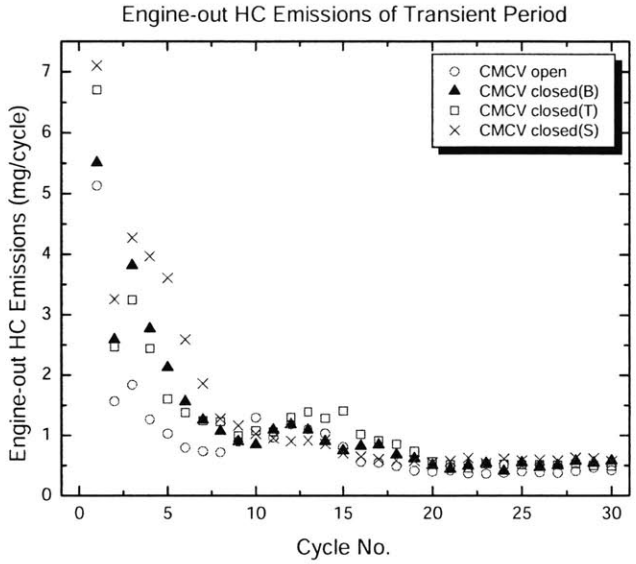

Figure 4-10 Engine-out HC mass emissions measured at the exhaust port exit of cylinder #4 as a function of cycle number during the transient period for various CMCVs.

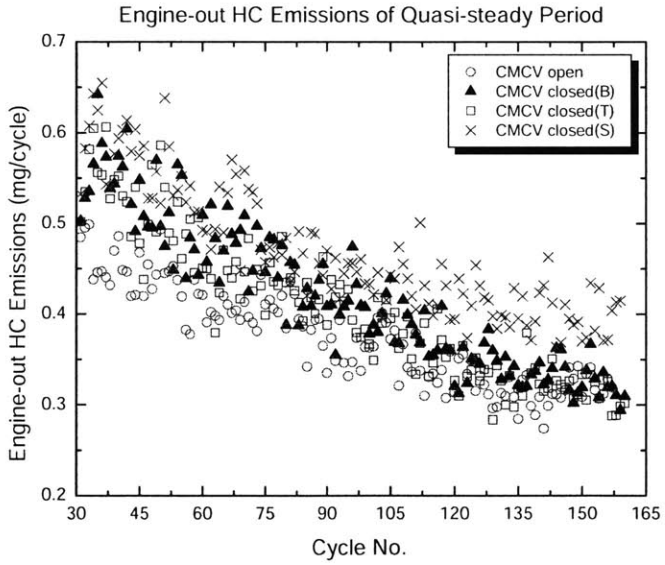

Figure 4-11 Engine-out HC mass emissions measured at the exhaust port exit of cylinder #4 as a function of cycle number during the quasi-steady period for various CMCVs.

4.2.5 Flow Testing Results

In order to quantify the in-cylinder charge motion with the CMCVs, flow bench tests were conducted at GM Powertrain Warren Engineering Center. The raw in-cylinder flow motion information, either the swirl or tumble, was indicated as a torque. However, the torques, by themselves, are of little value and must be corrected for flow rate and test conditions. By normalizing torque output values with engine geometries (bore and stroke) and plotting them versus valve lift, the swirl and tumble indexes were produced. Physically, the index represents a measure of the rate at which the charge in the cylinder is swirling or tumbling around its axis per engine revolution if all the inducted charge entered the cylinder at the given valve lift. More information about the swirl and tumble index calculation is described in Appendix A.3.

Figure 4-12 and 4-13 show the swirl and tumble index from the raw torque values that come from flow bench meters as a function of normalized valve lift. The strongest swirl flow was observed with the swirl type CMCV and the moderate increase of swirl flow was also shown with the base CMCV, while little impact on the swirl motion was identified with the tumble type CMCV. All three designs, however, increased the tumble index relative to the CMCV open case, and the base CMCV was found to give slightly higher tumble flow than the others.

The differences of these swirl and tumble motions are likely to affect the liquid fuel transport, distribution, and evaporation; therefore, those flow testing results can be correlated with the previous results of mixture preparation, combustion characteristics, and HC emissions.

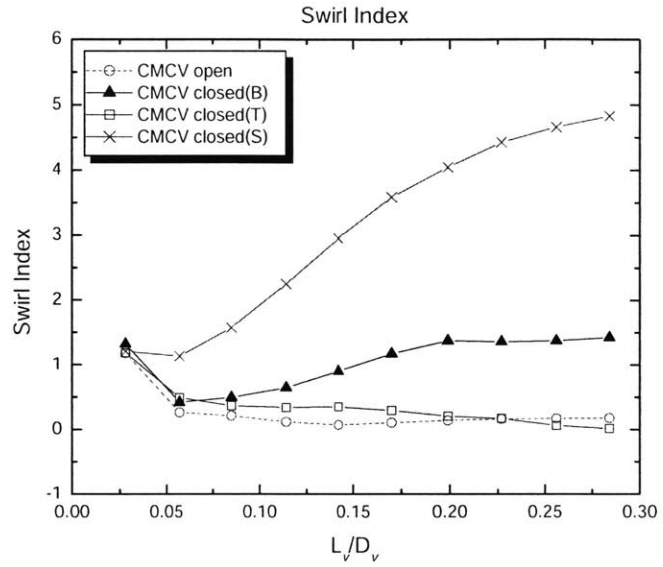

Figure 4-12 Swirl index from flow bench meters as a function of normalized valve lift for various CMCVs.

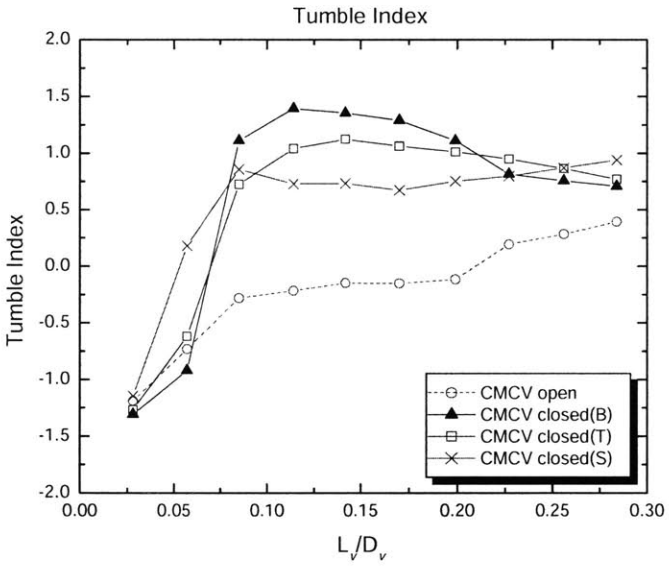

Figure 4-13 Tumble index from flow bench meters as a function of normalized valve lift for various CMCVs.

4.2.6 Overall Assessment of Different CMCVs

Different geometric charge motion control valves were found to yield differences in fuel evaporation, combustion rate, and engine-out HC emissions. With the same fuel injection and spark timing profile, the highest fuel evaporation was achieved with the base CMCV, which has the highest tumbling and also significant swirling flow motion. Lower fuel evaporation and higher HC emissions were observed with the swirl type CMCV, which has the strongest swirl motion and moderate tumble motion, than the other CMCVs. The swirl type CMCV showed slower 0-10% combustion but faster 10-90% combustion than the tumble type CMCV that enhances only the tumble motion.

A plausible mechanism can be developed by correlating the in-cylinder flow motion characteristics with the other results. With the swirl type CMCV, the bulk flow was forced to rotate strongly through the cylinder liner side; therefore, more of fuel droplets were presumably distributed near the cylinder wall than the centrally located spark plug gap. This was likely to cause the lack of fuel in the vicinity of spark plug gap and the excess of fuel near the cylinder wall. This fuel distribution can explain relatively slower flame initiation (0-10% combustion duration) in the earlier stage of combustion and higher flame propagation (10-90% combustion duration) in the later stage of combustion with the swirl type CMCV. In addition, by this excess swirl motion through the cylinder wall, more liquid fuel could wet the cylinder wall, resulting in increased amounts of fuel deposited in cylinder and also engine-out HC emissions. In contrast, with the tumble motion, strong flow patterns can be expected near the piston top and cylinder head surface. Thus, higher flow motion can be achieved in the vicinity of spark plug gap.

The overall results indicate that in-cylinder swirl and tumble motion should be appropriately combined by optimizing the shape of the CMCV. The base CMCV, which moderately enhanced the swirl and tumble motion, showed the greatest potential for mixture preparation, combustion characteristics, and HC emissions.

4.3 Effects of Reduced Fuel Injection

4.3.1 Modification of Fuel Injection

Since relatively richer in-cylinder mixture conditions were observed with the CMCV closed, reduced sequential fuel injection was then used with the CMCV closed case. In order to achieve the same in-cylinder lambda trace with the baseline CMCV open calibration, reduced amounts of fuel were injected for the CMCV closed case. Spark timings, however, were maintained at the same levels of the baseline CMCV open calibration. The impacts of spark timing on combustion and emissions were thus decoupled from the effects of reduced fuel injection.

The comparison of the various charge motion control valves indicates that the base CMCV has the greatest potential for improving mixture preparation and combustion characteristics even though it produces higher HC emissions (due mainly to the higher in-cylinder lambda conditions). Thus, the base CMCV was used for further comparison experiments.

4.3.2 Mixture Preparation

The effect of reduced fuel injection with the CMCV closed on mixture preparation was evaluated while using the same spark timing trace as the base CMCV open calibration. Figure 4-14 shows the injected fuel mass as a function of cycle number during the first 20 seconds following engine cranking, in order to obtain the same in-cylinder lambda trace as the baseline CMCV open calibration. The amount of cycle-by-cycle injected fuel mass was reduced approximately by 7.5% during the transient period, including a 12% reduction for the first two cycles. During the quasi-steady period, overall 3.5% less fuel was injected with the CMCV closed. Meanwhile, the same baseline spark timings were applied to both the CMCV open and closed case.

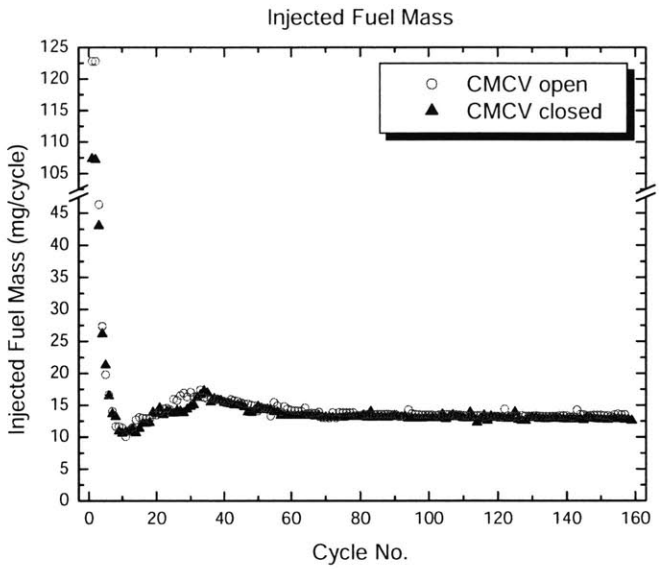

Figure 4-14 Required mass of injected fuel as a function of cycle number for the same in-cylinder lambda trace with the CMCV open and closed during the first 20 seconds after cranking commenced.

4.3.3 Combustion Characteristics

Combustion characteristics were investigated in terms of the variation of Net-IMEP and combustion duration in order to assess the effectiveness of the CMCV with reduced fuel injection. A smaller variation of Net-IMEP, shown in Figure 4-15, was obtained with the CMCV closed (relative to the CMCV open case) during the transient period, while the same in-cylinder lambda and spark timing trace were maintained. During the quasi-steady period, Net-IMEP averaged 2.45 bar with 5% COV for both the cases. Test-to-test variations in average Net-IMEP and COV were ±0.1 bar and ±0.3%, respectively.

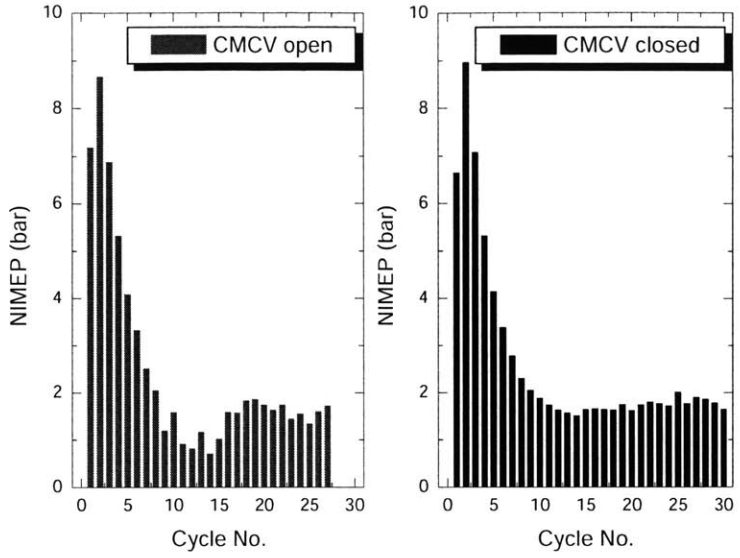

Figure 4-15 Net-IMEP as a function of cycle number during the transient period for the CMCV open case and the CMCV closed case with reduced fuel injection.

Burn rate analysis was performed on the first 20 seconds following engine cranking to determine the 0-10% and 10-90% combustion duration. Figure 4-16 and Figure 4-17 show clear differences between the CMCV open and closed case. Noticeable reductions in both the 0-10% and 10-90% combustion duration were found with the CMCV closed, especially during the transient period. Reduced combustion durations of the CMCV closed case could allow additional spark retard while injecting less fuel overall.

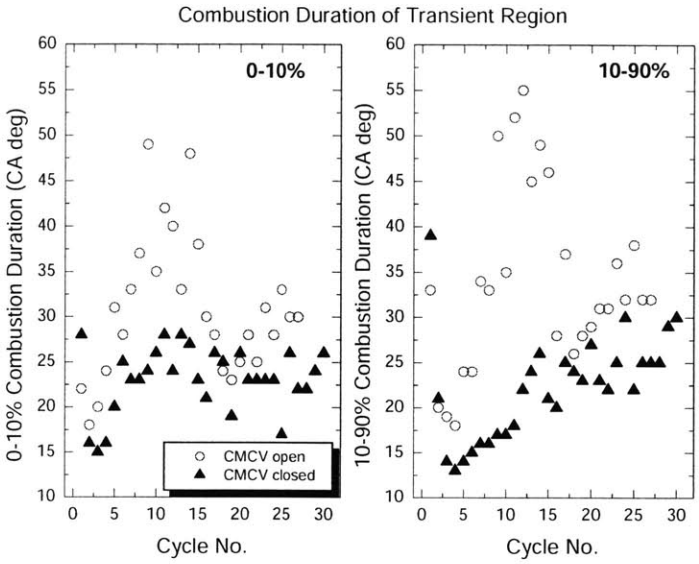

Figure 4-16 0-10% and 10-90% combustion durations as a function of cycle number during the transient period for the CMCV open case and the CMCV closed case with reduced fuel injection.

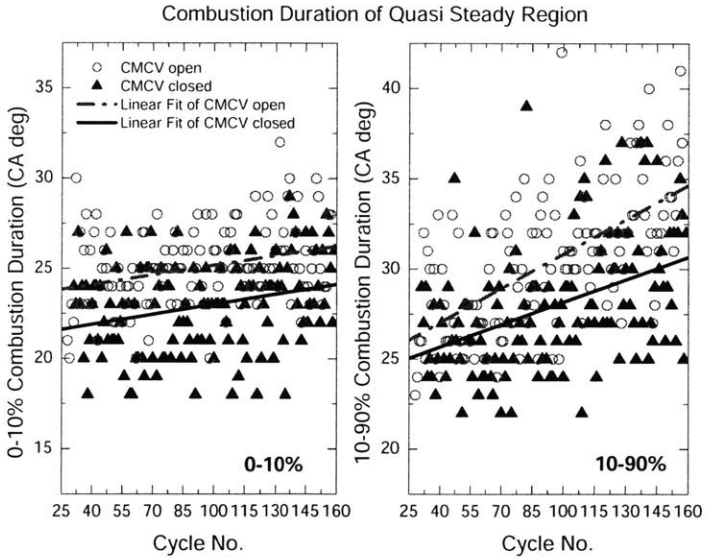

Figure 4-17 0-10% and 10-90% combustion durations as a function of cycle number during the quasi-steady period for the CMCV open case and the CMCV closed case with reduced fuel injection.

Gas motion effects on air-fuel mixture in the port and cylinder can be divided into two areas: the effect on mixture preparation which is represented by in-cylinder air/fuel ratio, and the effect on flame-development which is represented by the 0-10% energy-release fraction angle. Since the same in-cylinder lambda trajectory was maintained with the same spark timing for both the cases, the difference of the 0-10% combustion duration can be considered as the direct charge motion impact on flame-development. The CMCV thus decreased the 0-10% combustion duration, 8° CA on average during the transient period and 2° CA during the quasi-steady period, as a result of enhanced charge motion impacts on combustion initiation.

4.3.4 Exhaust Emissions

With the CMCV open, the high engine-out HC emissions region, shown in Figure 4-18, was observed near where the lowest intake manifold pressure occurred. The low in-cylinder pressure presumably assisted the vaporization of liquid fuel deposited throughout the engine. However, with the CMCV closed, high engine-out HC emissions were found in the earlier stages of engine start-up. This implies that the CMCV enhanced fuel evaporation rate right from the beginning; therefore, less liquid fuel should be deposited in the cylinder during the transient period. Figure 4-19 shows that the engine-out HC emissions during the quasi-steady period were reduced with the CMCV closed by 6.5%, while the same in-cylinder lambda and spark timing profile was maintained.

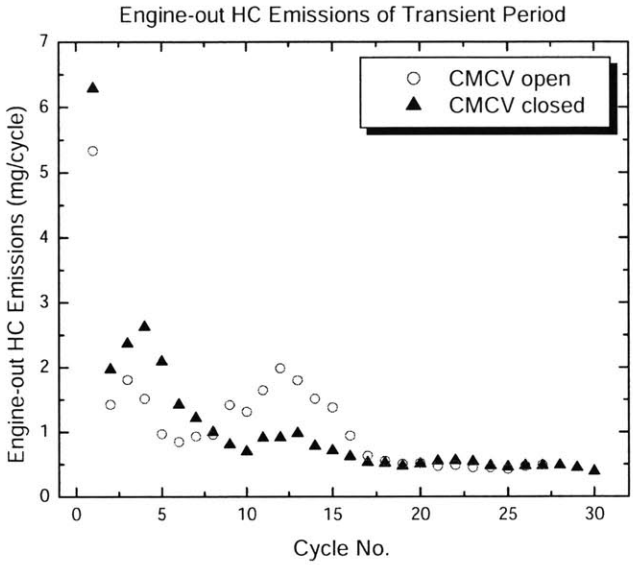

Figure 4-18 Engine-out HC mass emissions measured at the exhaust port exit of cylinder #4 as a function of cycle number during the transient period for the CMCV open case and the CMCV closed case with reduced fuel injection.

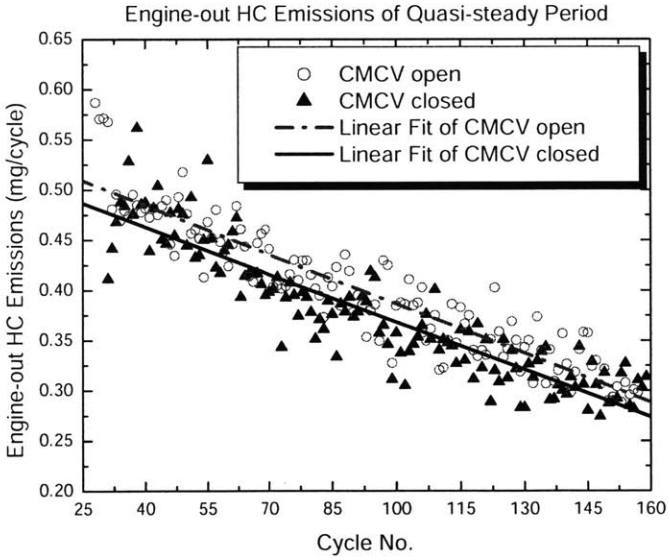

Figure 4-19 Engine-out HC mass emissions measured at the exhaust port exit of cylinder #4 as a function of cycle number during the quasi-steady period for the CMCV open case and the CMCV closed case with reduced fuel injection.

4.4 Effects of Retarded Spark Timing

4.4.1 Modification of Spark Timing

Since considerable shortening in combustion duration and improvement in combustion stability were achieved with the use of the charge motion control valve, additional spark retard was feasible with the CMCV closed. Three different spark modifications with the CMCV closed were investigated during the first 20 seconds following engine cranking. Spark timings, shown in Figure 4-20, were retarded ($\Delta\theta_{sp} = -5^{o}$ and -10^{o}) with respect to the baseline spark timing ($\Delta\theta_{sp} = 0^{o}$), while the same in-cylinder lambda trace was maintained for all three different spark modifications.

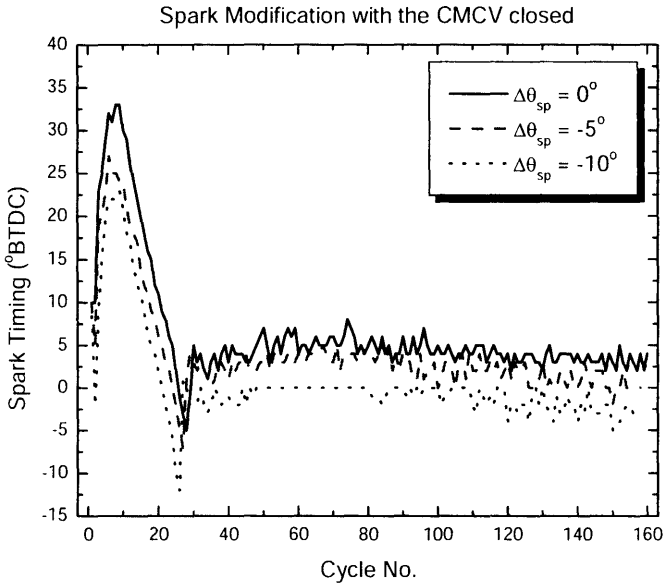

Figure 4-20 Spark timing as a function of cycle number during the first 20 seconds following engine cranking for various spark modifications with the CMCV closed.

4.4.2 Mixture Preparation

Figure 4-21 shows the required mass of injected fuel for the same in-cylinder lambda trace as the baseline spark timing ($\Delta\theta_{sp}$ = 0°) case. The steady-state experimental results showed that the air and fuel mass flow rates through the engine were increased with an increased level of spark retardation to maintain the same mean Net-IMEP. Similar trends were observed in the start-up experiments. As spark timing was retarded, more fuel was injected and also more air was inducted for the same in-cylinder lambda trajectory.

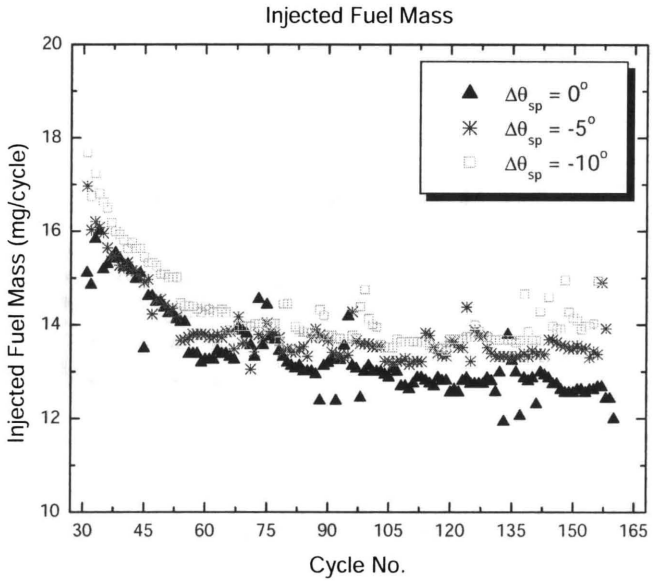

Figure 4-21 Required mass of injected fuel as a function of cycle number for the same in-cylinder lambda trace with various spark modifications during the first 20 seconds after cranking commenced.

4.4.3 Combustion Characteristics

As combustion was phased later in the cycle, spark timing retardation was limited by combustion stability. Therefore, at each of the three different spark modifications, combustion stability was assessed during the first 20 seconds following engine cranking. Figure 4-22 shows the Net-IMEP during the transient period. As the level of spark retardation was increased, there was a noticeable increase of fluctuation in the Net-IMEP during the transient period. During the quasi-steady period, the COV of Net-IMEP was also increased;

sient period. During the quasi-steady period, the COV of Net-IMEP was also increased; the COV of 5.2%, 6.0%, and 6.9% were observed for the $\Delta\theta_{sp} = 0^{o}$, $\Delta\theta_{sp} = -5^{o}$, and $\Delta\theta_{sp} = -10^{o}$ spark modification, respectively.

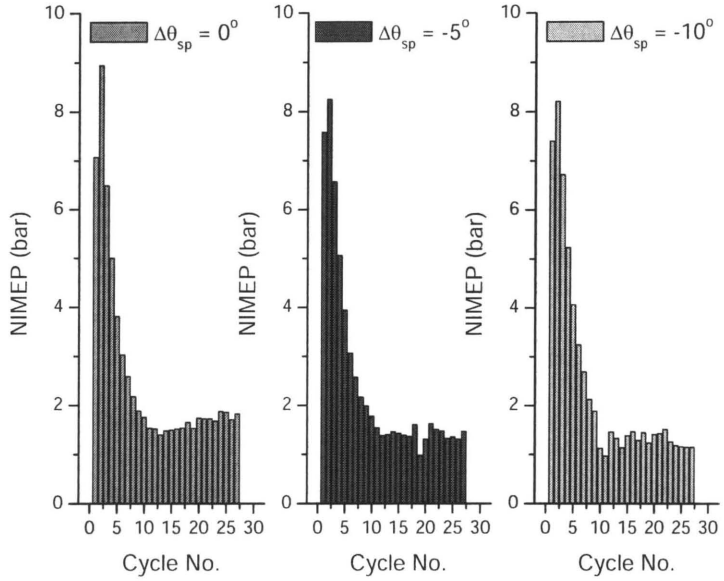

Figure 4-22 Net-IMEP as a function of cycle number during the transient period for various spark modifications with the CMCV closed.

The location of 50% mass fraction burned, 0-10% combustion duration and 10-90% combustion duration, shown in Figure 4-23, Figure 4-24 and Figure 4-25, were determined by burn rate analysis. As the spark timings were retarded, the locations of 50% mass fraction burned were also retarded during both the transient and quasi-steady period. With the most aggressive spark retardation ($\Delta\theta_{sp} = -10^{o}$), relatively larger variations in the location of 50% mass fraction burned and the 10-90% combustion duration were observed as combustion occurred in a rapidly expanding cylinder volume. However, relatively less variations were observed in the 0-10% combustion duration, which is influenced primarily by the in-cylinder mixture preparation and in-cylinder gas motion. This is likely because the in-cylinder lambda trace was fixed and gas motions in the vicinity of the spark plug were fairly similar due to the use of the CMCV for all three spark modifications.

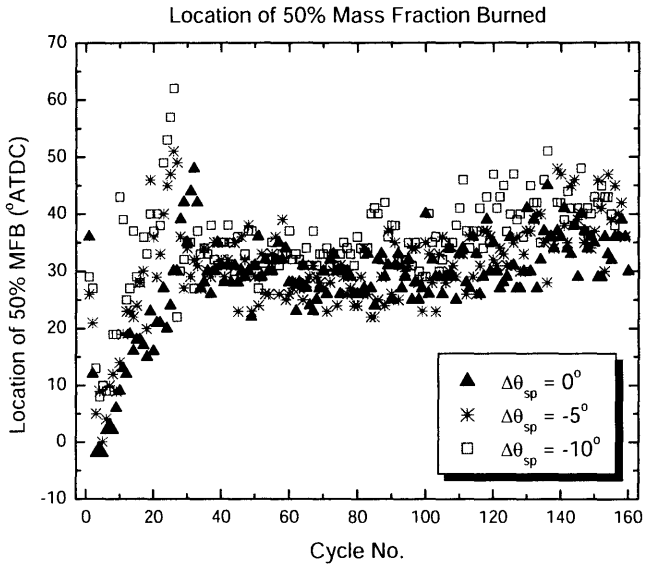

Figure 4-23 Location of 50% mass fraction burned as a function of cycle number during the 20 seconds after engine cranking for various spark modifications with the CMCV closed.

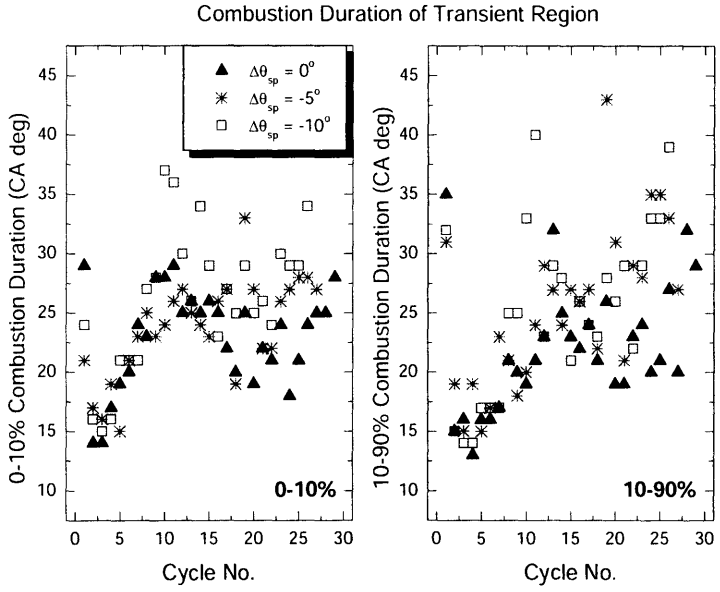

Figure 4-24 0-10% and 10-90% combustion durations as a function of cycle number during the transient period for various spark modifications with the CMCV closed.

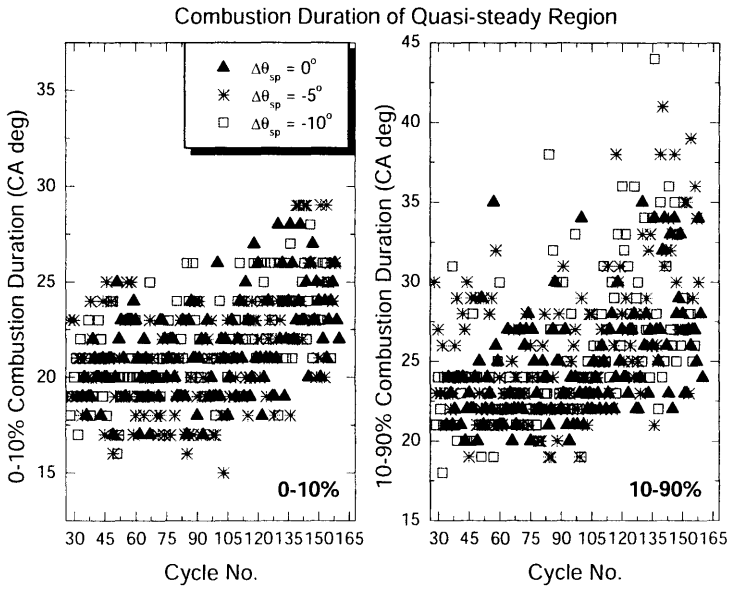

Figure 4-25 0-10% and 10-90% combustion durations as a function of cycle number during the quasi-steady period for various spark modifications with the CMCV closed.

4.4.4 Exhaust Emissions

Time-resolved cylinder #4 exhaust port exit HC, CO and CO_2 concentration measurements were taken for the first 20 seconds of engine operation. In order to investigate the effect of retarded spark timing, the engine-out HC mass emissions were evaluated for three different spark modifications. Figure 4-26 and Figure 4-27 show that the engine-out HC emissions were reduced with the moderate spark retardation ($\Delta\theta_{sp} = -5^{\circ}$) by 22% during the transient period and by 14% during the quasi-steady period. However, with the more aggressive spark retardation ($\Delta\theta_{sp} = -10^{\circ}$), the engine-out HC emissions were increased by 20% during the transient period and by 14% during the quasi-steady period. As described in Section 4.4.2, the air and fuel mass flow rates through the engine were increased with increased levels of spark retardation to maintain the same mean Net-IMEP. Thus, a decrease in HC concentrations with the spark retardation was more than offset by an increase in mass flow rate.

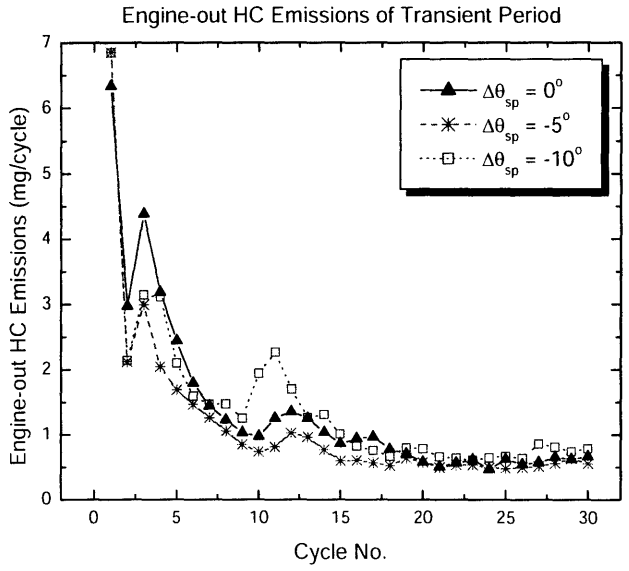

Figure 4-26 Engine-out HC mass emissions measured at the exhaust port exit of cylinder #4 as a function of cycle number during the transient period for various spark modifications with the CMCV closed.

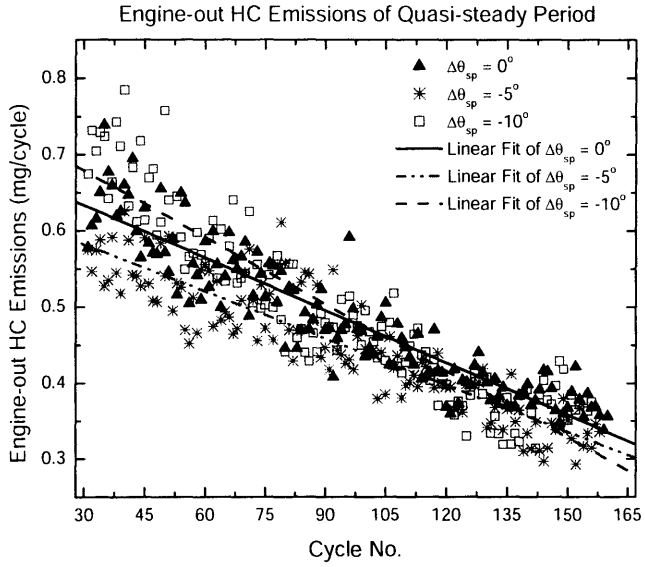

Figure 4-27 Engine-out HC mass emissions measured at the exhaust port exit of cylinder #4 as a function of cycle number during the quasi-steady period for various spark modifications with the CMCV closed.

4.5 Modified Start-up Strategy with CMCV closed

4.5.1 Modification of Fuel Injection and Spark Timing

As discussed in the previous sections, mixture preparation and combustion characteristics were improved with the CMCV closed by enhancing fuel vaporization and increasing burning rate. Greater fuel vaporization allowed reduced fuel injection and the faster burning rate enabled additional spark retard. In addition, the extended retardation of spark timing decreased HC emissions. Therefore, an appropriate combination of reduced fuel injection and retarded spark timing with the CMCV closed could be a way to achieve more robust combustion and lower HC emissions during the engine start-up process.

In order to achieve the same in-cylinder lambda profile as the baseline CMCV open calibration, reduced sequential fuel injection strategy was applied to the CMCV closed case as shown in Figure 4-28. The amount of reductions in fuel injection was determined by the results of Section 4.3. At the same time, retarded spark timing strategy was also utilized to the CMCV closed case for more reductions in HC emissions as shown in Figure 4-29. Spark timing was modified using the results of Section 4.3 and Section 4.4.

During the transient period (0 to 3 seconds), a total of 7.5% reduced fuel, including a 12% reduction for the first two cycles, and 8° CA retarded spark timing were applied to the CMCV closed case. During the quasi-steady period (3 to 20 seconds), overall 3.5% reduced fuel and 5° CA retarded spark timing were applied to the CMCV closed case with respect to the baseline CMCV open case.

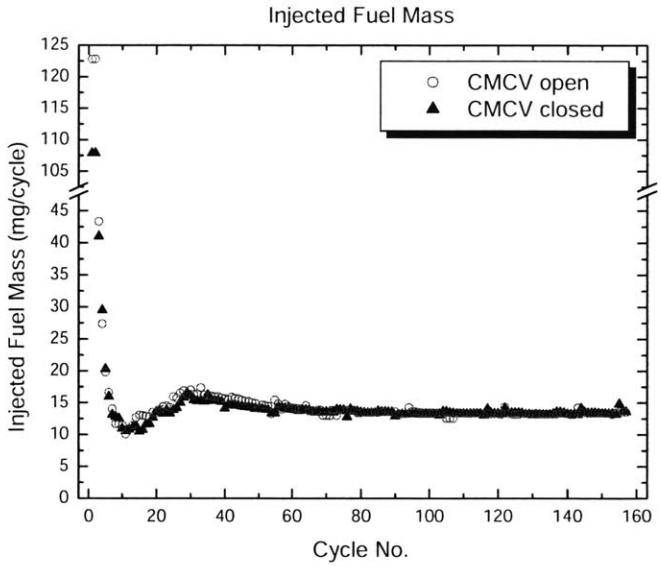

Figure 4-28 Injected fuel mass as a function of cycle number with the CMCV open and closed during the first 20 seconds after cranking. Reduced sequential fuel injection strategy was applied to the CMCV closed case.

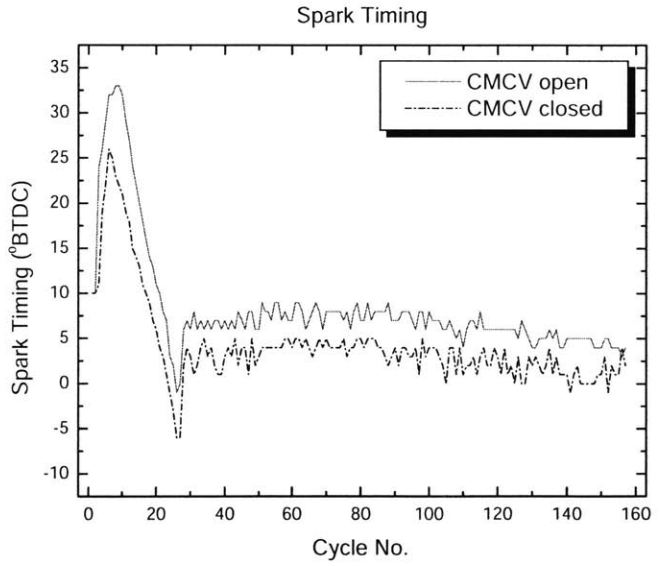

Figure 4-29 Spark timing as a function of cycle number with the CMCV open and closed during the first 20 seconds after cranking. Retarded spark timing strategy was applied to the CMCV closed case.

4.5.2 Mixture Preparation

In-cylinder lambda was calculated from the exhaust HC, CO, and CO_2 emissions data to investigate mixture preparation before combustion. Figure 4-30 shows in-cylinder lambda traces as a function of cycle number for the cases described in the previous section. Cycle-by-cycle in-cylinder lambda points were well matched for both cases within ±2%. Figure 4-30 suggests that both cases had similar mixture preparation conditions before combustion occurred.

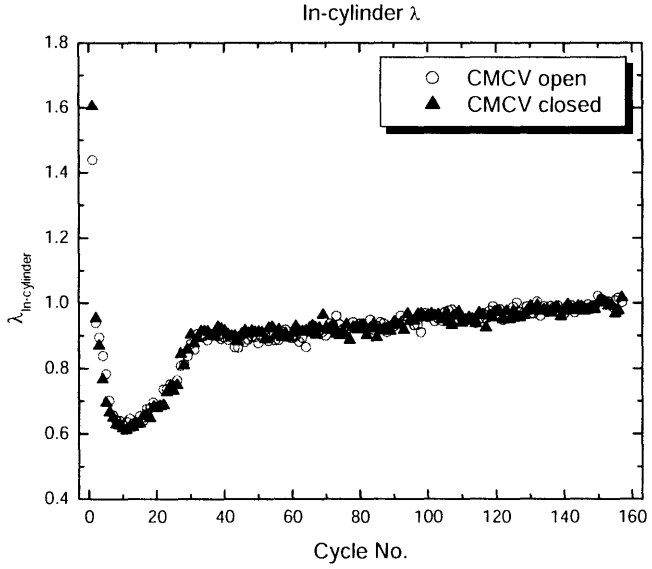

Figure 4-30 In-cylinder λ as a function of cycle number during the first 20 seconds following engine cranking with the CMCV open and closed. Reduced sequential fuel injection and retarded spark timing strategy was applied to the CMCV closed case.

4.5.3 Combustion Characteristics

Net-IMEP and combustion durations were calculated from in-cylinder pressure data acquired from cylinder #4 in order to investigate combined effects of reduced fuel and retarded spark timing with enhanced charge motion on combustion characteristics. Qualitative observation of Net-IMEP shown in Figure 4-31 indicates that combustion stability was improved with the CMCV closed during the transient period. However, the COV of Net-

IMEP during the quasi-steady period was increased by about 1%; the COV of 5% and 6% were observed for the CMCV open and closed case, respectively.

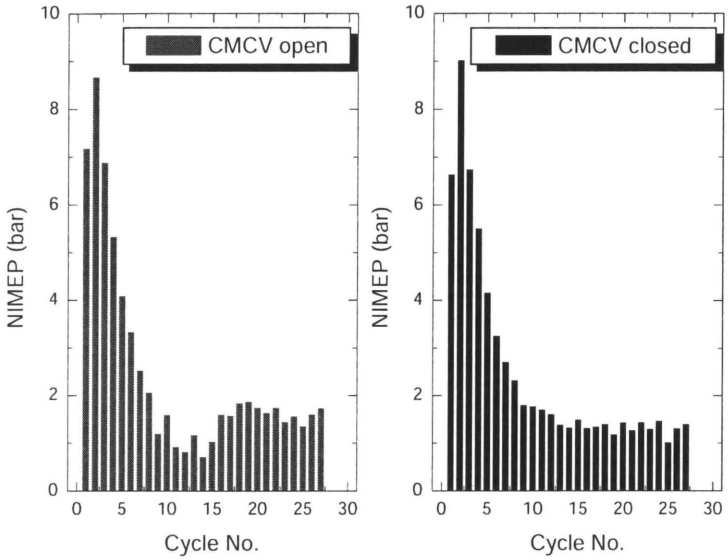

Figure 4-31 Net-IMEP as a function of cycle number during the transient period with the CMCV open and closed. Reduced sequential fuel injection and retarded spark timing strategy was applied to the CMCV closed case

Burn rate analysis was conducted on the first 20 seconds following engine cranking. Figure 4-32 and 4-33 show a comparison of the 0-10% and 10-90% combustion duration and the location of 50% mass fraction burned during the transient period. Significantly reduced combustion duration was achieved with CMCV closed even using 7.5% less fuel and 8^{o} CA spark retardation. The location of 50% mass fraction burned shown in Figure 4-33 was also advanced especially between cycle number 5-15 where intake manifold pressure has severely low values. Since the location of 50% mass fraction burned gives a good indication of when combustion is occurring, the results shown in Figure 4-33 suggests possible additional spark retardation with the CMCV closed during the transient period.

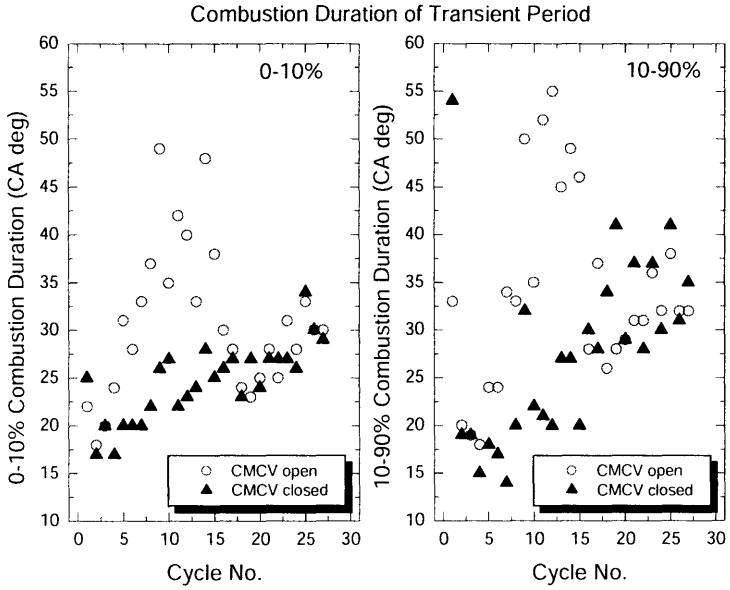

Figure 4-32 0-10% and 10-90% combustion durations as a function of cycle number during the transient period with the CMCV open and closed. Reduced sequential fuel injection and retarded spark timing strategy was applied to the CMCV closed case.

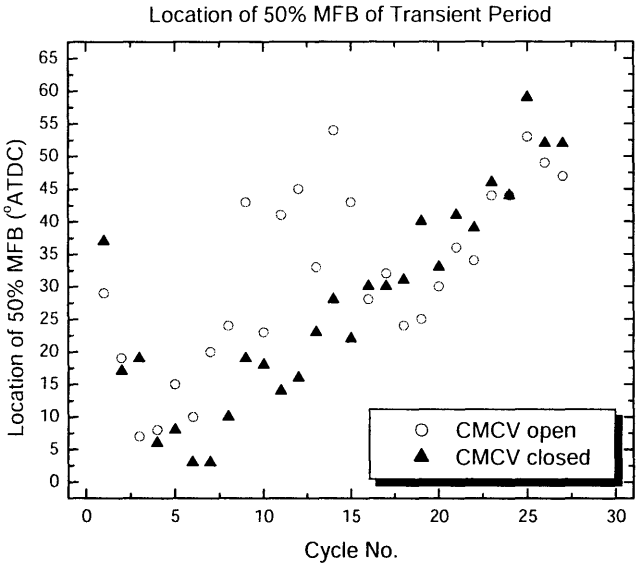

Figure 4-33 Location of 50% mass fraction burned as a function of cycle number during the transient period with the CMCV open and closed. Reduced sequential fuel injection and retarded spark timing strategy was applied to the CMCV closed case.

Figure 4-34 and 4-35 show a comparison of the 0-10% and 10-90% combustion duration and the location of 50% mass fraction burned during the quasi-steady period. Relatively large variations in the 10-90% combustion duration and the location of 50% mass fraction burned were observed with CMCV closed. This increased variation was responsible for slightly decreased combustion stability (COV) during the quasi-steady period. Variations in the location of 50% mass fraction burned are known as the primary cause of cyclic variations in the Net-IMEP. Since the expansion ratio decreases rapidly during combustion for retarded spark timing, the combustion phasing is one of the major factors which determines individual cycle Net-IMEP. Both the CMCV open and closed case were found to experience almost the same combustion phasing on average since two linear fit lines of the location of 50% mass fraction burned almost coincided, while using reduced sequential fuel injection and retarded spark timing strategy for the CMCV closed case.

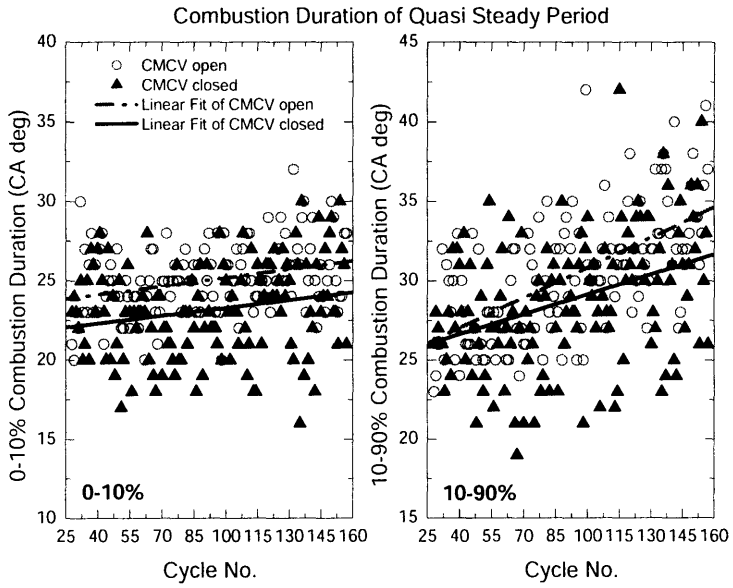

Figure 4-34 0-10% and 10-90% combustion durations as a function of cycle number during the quasi-steady period with the CMCV open and closed. Reduced sequential fuel injection and retarded spark timing strategy was applied to the CMCV closed case.

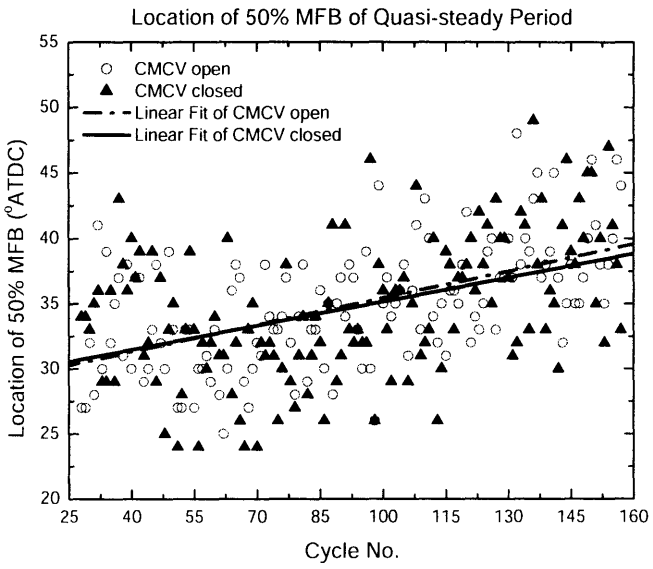

Figure 4-35 Location of 50% mass fraction burned as a function of cycle number during the quasi-steady period with the CMCV open and closed. Reduced sequential fuel injection and retarded spark timing strategy was applied to the CMCV closed case.

4.5.4 Exhaust Emissions

HC, CO and CO_2 concentrations were measured at the exhaust port exit of cylinder #4 during the first 20 seconds after engine cranking commenced. Figure 4-36 and Figure 4-37 show the mass of engine-out HC emissions per cycle during the transient period and during the quasi-steady state, respectively. There was a noticeable decrease in engine-out HC emissions around the region in which the intake manifold pressure was lowest. The engine-out HC emissions were reduced by 18% during the transient period and by 7% during the quasi-steady period. A total reduction of 12% in HC emissions was achieved by the charge motion control valve with the reduced fuel injection and retarded spark timing.

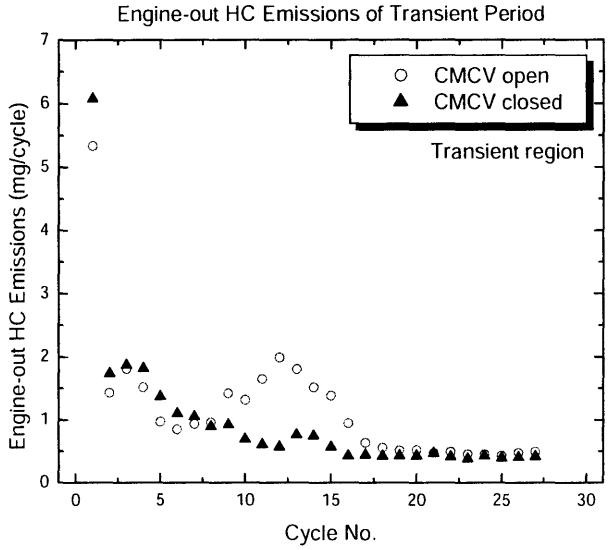

Figure 4-36 Engine-out HC mass emissions measured at the exhaust port exit of cylinder #4 as a function of cycle number during the transient period with the CMCV open and closed. Reduced sequential fuel injection and retarded spark timing strategy was applied to the CMCV closed case.

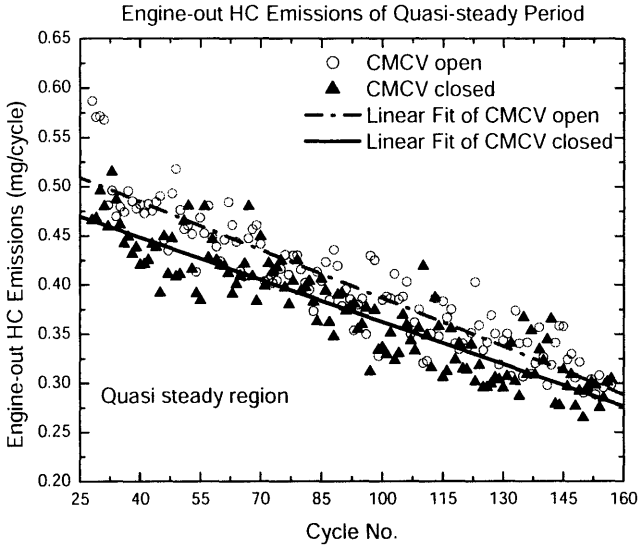

Figure 4-37 Engine-out HC mass emissions measured at the exhaust port exit of cylinder #4 as a function of cycle number during the quasi-steady period with the CMCV open and closed. Reduced sequential fuel injection and retarded spark timing strategy was applied to the CMCV closed case.

Chapter 5

Summary, Conclusions, and Recommendations

5.1 Overview

The purpose of this research was to investigate the effects of various intake charge motion control approaches on the cold start-up process of a port fuel injected SI engine. Experiments were performed to assess the effectiveness of enhanced charge motion on mixture preparation, combustion, and HC emissions. In this chapter, the findings of the research will be summarized, conclusions will be drawn, and implications for future research will be discussed.

5.2 Steady State Experiments

Steady state experiments were conducted to provide basic insight into combustion characteristics and HC emissions behavior with the charge motion control valve (CMCV). The combustion process and exhaust gas state were examined under the fixed engine operation (2.5 bar Net-IMEP, 1000 rpm) and cold (20°C) fluid condition. The following conclusions were obtained from the steady state experimental results.

- Increased charge motion with the CMCV closed was found to shorten the 0-10% and 10-90% combustion duration at a given spark timing. This reduced combustion duration caused the 50% mass fraction burned to occur up to 5° CA earlier for the same spark timing.

- With increased spark retardation from optimum timing, combustion stability was found to worsen as more of the combustion process occurred in a rapidly expanding cylinder volume. However, significant improvements in combustion stability (0.5-1.5% reductions in COV) were achieved with the CMCV closed as spark timing was retarded. This is due to the increase in burn rate with the CMCV closed, resulting from the higher in-cylinder velocity and turbulence.

- The CMCV decreased the exhaust gas temperature between 5-30°C at a given spark timing, which was attributed to the increased in-cylinder heat transfer during combustion due to the effectively less retarded combustion phasing (location of 50% mass fraction burned) with the CMCV closed. However, at equivalent levels of combustion phasing, there was close agreement between the CMCV open and closed exhaust gas temperatures.

- No noticeable advantage on the exhaust HC emissions was found with the CMCV closed at an equivalent combustion phasing in steady state idle operation, since the exhaust HC mass flow rate with the CMCV closed was almost coincident with the CMCV open case. This is mainly due to faster combustion and slightly higher peak pressure, which have offsetting effects on the various sources of HC within the cylinder.

- The use of the CMCV improved fuel consumption at retarded spark timings. Improvements in ISFC were obtained with the CMCV closed due to enhanced air-fuel mixing and relatively faster burning, which caused the earlier end of combustion. The ISFC at a given spark timing was reduced up to 8% relative to the CMCV open case, as spark timing was retarded.

5.3 Engine Start-up Experiments

Engine start-up experiments were conducted with the three different geometric charge motion control valves. Mixture preparation, combustion characteristics, and HC emissions were evaluated with the various fuel injection and spark timing strategies during the first 20

seconds following engine cranking. The engine operation was divided into two distinct periods (transient period and quasi-steady period) at about 3 seconds, after which the engine entered into the quasi-steady idle operation. The following conclusions were based on the results of those engine start-up experiments.

Effects of the CMCV with the same fuel injection and spark profile

- The use of the CMCV was found to improve mixture preparation during the engine start-up process. With the same fuel injection and spark timing trajectory, the CMCV increased the amount of fuel evaporated relative to the CMCV open case. This is mainly due to higher mixture velocities through the upper part of valve, which increases atomization of liquid fuel at the valve seat, resulting in finer fuel droplets and more rapid distribution and mixing with hot residual gas.

- Significant differences were observed between the different geometric charge motion control valves. The highest evaporation rate was obtained from the swirl-tumble type CMCV (base type CMCV as shown in Figure 4-3). The liquid fuel transport, distribution, and evaporation were affected by the combined swirl and tumble flow motion, and correlated with combustion characteristics and HC emissions. Moderately enhanced swirl and tumble motion, which was produced by the base CMCV, showed the greatest potential for improving mixture preparation, combustion characteristics, and HC emissions.

Effects of the CMCV with reduced fuel injection under the same spark profile

- The same in-cylinder air/fuel ratio profile as the CMCV open case was achieved with the CMCV closed by injecting 7.5% less fuel during the transient period (0 to 3 seconds) and 3.5% less fuel during the quasi-steady period (3 to 20 seconds) due to improved fuel transport and evaporation, while the same spark timing trajectory was maintained.

- Charge motion impact on initial flame development was assessed by comparing the burn rate analysis results with the same in-cylinder air/fuel ratio and spark timing profile. The 0-10% combustion duration was reduced by 8° CA on average during the transient period and 2° CA during the quasi-steady period due to enhanced in-cylinder charge motion resulting from the use of the CMCV. Significant reductions in the combustion duration were found with the CMCV closed, especially during the transient period.

- Using the CMCV with the same in-cylinder lambda and spark timing profile, peak engine-out HC emissions (excluding the first cycle) occurred in the earlier stages of engine start-up process relative to the CMCV open case. Combining this with the fact that the same burned fuel mass trajectory was maintained indicates that the CMCV enhanced liquid fuel transport and evaporation rates, resulting in less liquid fuel being deposited in the cylinder during the transient period. The engine-out HC emissions during the quasi-steady period were reduced with the CMCV closed by 6.5%.

Effects of the CMCV with retarded spark under the same fuel injection profile

- Reduced combustion duration with the CMCV closed enabled additional spark retard while injecting less fuel overall. Combustion stability worsened as combustion was phased later. Moderate spark retard ($\Delta\theta_{sp}$ = -5°) was found to reduce the engine-out HC emissions by 22% during the transient period and by 14% during the quasi-steady period relative to the baseline spark timing ($\Delta\theta_{sp}$ = 0°). HC emissions decreased at retarded spark timings due to decreased crevice volume fraction at peak pressure and increased burned gas temperatures at the end of the expansion and during exhaust, which increased post combustion oxidation.

Effects of the CMCV with reduced fuel injection and retarded spark profile

- The same in-cylinder air/fuel ratio profile as the baseline CMCV open case was achieved with the CMCV closed by applying 7.5% reduced fuel and 8° CA spark re-

tard for the transient period and 3.5% reduced fuel and 5° CA spark retard for the quasi-steady period due to increased fuel vaporization and burning rates.

- By the combination of reduced fuel injection and retarded spark timing strategy with the CMCV closed, the combustion stability was increased during the transient period. However, the COV of Net-IMEP during the quasi-steady period was worsened from about 5% to 6%.

- A total reduction of 12% in HC emissions during the first 20 seconds of operation was achieved by the charge motion control valve with the reduced fuel injection and retarded spark timing. The engine-out HC emissions were reduced by 18% during the transient period and by 7% during the quasi-steady period. This improvement was mainly influenced by enhanced liquid fuel transport into the cylinder and increased fuel vaporization, which allowed reduced fuel injection and prevented liquid fuel deposited within the cylinder.

5.4 Overall Assessment and Recommendations

- The CMCV was found to improve the engine's cold start-up characteristics. In particular, greater improvement in mixture preparation, combustion stability, and HC emissions were observed during the initial 3 seconds (transient period) before the engine reached quasi-steady idle operation.

- Considering that a large fraction of the total HC emissions during the Federal Test Procedure (FTP) is emitted during the first 20 seconds, and also that approximately 40% of the first 20 second HC emissions are emitted during the first 3 seconds, it would be beneficial to use the charge motion control valve even for the first 3 seconds of engine cold start-up.

- Different shape charge motion control valves, which produced different in-cylinder flows, were found to yield the differences in fuel evaporation, combustion rate, and engine-out HC emissions due to the combined effects of the swirl and tumble mo-

tion. Flow testing results indicate that better performance was obtained with the CMCV geometries that produced moderate swirl and tumble intensities rather than high swirl or tumble alone

- Greater fuel vaporization and faster burning rate with the CMCV closed allowed reduced fuel injection and additional spark retard, resulting in a significant reduction in HC emissions during the engine cold start-up process.

- Since less liquid fuel deposits within the cylinder in the early stage of engine start-up with the CMCV closed, more precise cycle-by-cycle fuel metering, which is required for the low emissions engine start-up, can be achieved for the first hundred cycles by the use of the CMCV.

References

References

1. Heywood, J.B., *Internal Combustion Engine Fundamentals*, McGraw-Hill, New York, 1988.
2. Cheng, W.K., Hamrin D., Heywood, J.B., Hochgreb, S., Min, K., and Norris, M., "An overview of hydrocarbon emissions mechanisms in spark-ignition engines", SAE Paper 932708, 1993.
3. Takeda, K., Yaegashi, T., Sekiguchi, K., Saito, K., and Imatake, N., "Mixture preparation and HC emissions of a 4-valve engine during cold starting and warm-up", SAE Paper 950074, 1995.
4. Cheng, W.K. and Santoso, H., "Mixture preparation and hydrocarbon emissions behaviors in the first cycle of SI engine cranking", SAE Paper 2002-01-2805, 2002.
5. Meyer, R. and Heywood, J.B., "Evaporation of in-cylinder liquid fuel droplets in an SI engine: A diagnostic-based modeling study", SAE Paper 1999-01-0567, 1999.
6. Henein, N.A., Tagomori, M.K., Yassine, M.K., Asmus, T.W., Thomas, C.P., and Hartman, P.G., "Cycle-by-cycle analysis of HC emissions during cold start of gasoline engines", SAE Paper 952402, 1995.
7. Castaing, B.M., Coward, J.S., and Cheng, W.K., "Fuel metering effects on hydrocarbon emissions and engine stability during cranking and start-up in a port fuel injected spark ignition engine", SAE Paper 2000-01-2836, 2000.
8. Takahashi, H., Ishizuka, Y., Tomita, M., and Nishizawa, K., "Engine-out and tail-pipe emission reduction technologies of V-6 LEVs", SAE Paper 980674, 1998.
9. Nishizawa, K., Momoshima, S., Koga, M., and Tsuchida, H., "Development of new technologies targeting zero emissions for gasoline engines", SAE Paper 2000-01-0890, 2000.
10. Jung, H.H., Stein, R.A., and Leone, T.G., "Comparison of dual retard VCT to continuously variable event valvetrain", SAE Paper 2004-01-1268, 2004.
11. Development Instrumentation Group, *Delco Modular Development System Manual,* Delco Electronics Corporation, 1997.

12. Cambustion HFR400, April 2005
<http://www.cambustion.co.uk/instruments/hfr400>.
13. Cambustion NDIR500, April 2005
<http://www.cambustion.co.uk/instruments/ndir500/ndirprinciples.html>.
14. UTG-91 Fuel Properties, Chevron Phillips Chemical Company LLC, October 2004
<http://www.cpchem.com/enu/tds_unsecured/UTG-91.pdf>.
15. Klein, D. and Cheng, W.K., "Spark ignition engine hydrocarbon emissions behaviors in stopping and restarting", SAE Paper, 2002-01-2804, 2002.
16. Fox, J.W., Cheng, W.K., and Heywood, J.B., "A model for predicting residual gas fraction in spark-ignition engines", SAE Paper 931025, 1993.
17. Cheung, H.M. and Heywood, J.B., "Evaluation of a one-zone burn-rate analysis procedure using production SI engine pressure data", SAE Paper 932749, 1993.

Appendix A

A.1 Energy Release Equation

$$\frac{\partial Q_{CH}}{\partial \theta} = \frac{\gamma - 1}{\gamma} p \frac{\partial V}{\partial \theta} + \frac{1}{\gamma - 1} V \frac{\partial p}{\partial \theta} + \frac{\partial Q_{CR}}{\partial \theta} + \frac{\partial Q_{HT}}{\partial \theta}$$

where:

Q_{CH}	fuel chemical energy
θ	crank angle
γ	ratio of specific heat
p	cylinder pressure
V	cylinder volume
Q_{CR}	energy in crevices
Q_{HT}	heat transfer

A.2 Residual Gas Fraction Calculation

Fox Model (modified for a 4-valve engine)

$$x_r = 1.266 \cdot \frac{OF}{N} \cdot \left(\frac{P_i}{P_e} \right)^{-0.87} \cdot \sqrt{|P_e - P_i|} + 0.632 \cdot \phi \cdot \frac{(P_i / P_e)^{-0.74}}{r_c}$$

$$OF = \frac{1.45}{B} \cdot (107 + 7.8 \cdot \Delta\theta + \Delta\theta^2) \cdot \left(\frac{L_{v,\max} \cdot D_v}{B^2} \right)$$

A.3 Swirl and Tumble Index

Swirl Index (SI) :

This is an estimate of the swirl number if the cylinder was filled at this valve lift and there were no effects of compressibility.

$$SI = \frac{2\tau_s S \rho_{cyl}}{\pi^2} \frac{\pi^2}{8}$$

Note: The term ($\pi^2/8$) is to correct for "mass weighting" of the mean piston speed when assigning an engine speed to match the flow rate of the steady flow bench.

SI = swirl index

τ_s = swirl torque on honeycomb element (N·mm)

S = engine stroke (mm)

ρ_{cyl} = in-cylinder density at test conditions (kg/m^3)

Calculate ρ_{cyl} from the ideal gas relation:

$$\rho_{cyl} = \frac{1000\, p_D}{288.17 T_D} \left(kg/m^3\right)$$

Note: This equation assumes the gas pressure and temperature at the valve-exit-plane are the same as those within the cylinder.

p_D and T_D are pressure and temperature in the cylinder at each test point.

Tumble Index (TI) :

This is an estimate of the tumble number if the cylinder was filled at this valve lift and there were no effects of compressibility.

$$TI = \frac{2\tau_{cor} S \rho_{cyl}}{n\omega^2} \frac{\pi^2}{8}$$

Note: The term ($\pi^2/8$) is to correct for "mass weighting" of the mean piston speed when assigning an engine speed to match the flow rate of the steady flow bench.

TI = tumble index

S = engine stroke (mm)

τ_{cor} = corrected torque (N·mm)

ρ_{cyl} = in-cylinder density at test conditions (kg/m^3)

Calculate τ_{cor}:

$$\tau_{cor} = \tau_{meas} \frac{2}{1 + \frac{1}{3}\left(\frac{20S}{9B}\right)^2} CAL$$

Second term in correction equation is to convert from the moment of inertia for a cylinder about its axis into the moment of inertia for a cylinder rotated about a central diameter.

S = engine stroke (mm)

B = engine bore (mm)

τ_{meas} = measured torque (N·mm)

τ_{cor} = corrected torque (N·mm)

CAL = calibration factor to account for fraction of tumble angular momentum intercepted and measured by sensing element. Current best estimate of calibration to use for WEC fixture is 1.0.